



Fretting Fatigue in Mechanical Joints: A Literature Review

Dario Croccolo, Massimiliano De Agostinis, Stefano Fini, Giorgio Olmi, Francesco Robusto and Chiara Scapecchi *

Department of Industrial Engineering, University of Bologna, Viale del Risorgimento 2, 40136 Bologna, Italy; dario.croccolo@unibo.it (D.C.); m.deagostinis@unibo.it (M.D.A.); stefano.fini@unibo.it (S.F.); giorgio.olmi@unibo.it (G.O.); francesco.robusto@unibo.it (F.R.)

* Correspondence: chiara.scapecchi@unibo.it

Abstract: Fretting fatigue is a fatigue damage process that occurs when two surfaces in contact with each other are subjected to relative micro-slip, causing a reduced fatigue life with respect to the plain fatigue case. Fretting has now been studied deeply for over 50 years, but still no univocal design approach has been universally accepted. This review presents a literature study that involves the three main types of mechanical joint affected by fretting fatigue (press-fitted shaft hub joints, dovetail joints, and bolted joints) aiming at giving insight into the progress made in terms of design guidelines for engineers.

Keywords: fretting fatigue; fretting; bolted joint; interference fit; dovetail joint

Citation: Croccolo, D.; De Agostinis, M.; Fini, S.; Olmi, G.; Robusto, F.; Scapecchi, C. Fretting Fatigue in Mechanical Joints: A Literature Review. *Lubricants* **2022**, *10*, 53. <https://doi.org/10.3390/lubricants10040053>

Received: 19 February 2022

Accepted: 27 March 2022

Published: 30 March 2022

Publisher's Note: MDPI stays neutral with regard to jurisdictional claims in published maps and institutional affiliations.



Copyright: © 2022 by the authors. Licensee MDPI, Basel, Switzerland. This article is an open access article distributed under the terms and conditions of the Creative Commons Attribution (CC BY) license (<http://creativecommons.org/licenses/by/4.0/>).

1. Introduction

Fretting is a phenomenon that occurs when two contacting surfaces are subjected to oscillating tangential forces. Zones of microslip develop along the contact surface where sliding occurs, leading to considerable surface damage. As a result, two main effects can be observed:

- Wear of the surfaces;
- A considerable reduction in fatigue life.

If there is a predominance of the former effect, the phenomenon that occurs is called fretting wear, and vice versa with fretting fatigue taking place. This second phenomenon is perhaps more dangerous because it has been responsible for many critical service failures of components, leading sometimes to tragic accidents.

Generally speaking, the fretting damage process can be divided into three different phases, as reported by Hurricks [1]. The first phase deals with the removal of the oxide layer on the contact surfaces due to the mechanical wear. After the first few fretting cycles, the oxide layer has been completely worn off and the underlying component materials start to adhere, with the consequent development of micro welds and an increase in the coefficient of friction. Additional loading cycles cause the micro welds to break, forming wear debris [2]. More fretting cycles entail plastic deformation and microcrack development near the surface, further wear and possibly formation of new oxide, both on the component materials and on the wear particles. These cracks develop in correspondence to the stress concentration at the contact edge, namely the boundary with the non-slip area. The existence of non-propagated fretting cracks has been reported [3,4], suggesting that while fretting might heavily influence crack initiation and initial growth, the eventual crack growth far from the contact area is dominated by sufficiently high stress fields as in normal fatigue. The fretting problem is closely connected with the different types of contact [5]: in incomplete contacts, the contact area is strictly connected to the normal load, whilst in complete contacts, stress singularities are introduced in correspondence to sharp corners. It is known that the increasing residual shearing

tractions in frictional complete contacts further restricts sliding during the fretting cycles [6,7]. The same effect does not occur in incomplete contacts and therefore local sliding will always occur, making this kind of contact more inclined to fretting fatigue. In order to better understand the fretting phenomenon, it is therefore crucial to understand the different contact conditions and, therefore, a short review of contact mechanics analytical studies is presented.

1.1. Contact Mechanics

The first analytical study of contact was presented in 1882 by Hertz [8]. Theoretically, when two non-conforming bodies are naturally placed in contact, the contact zone is a point or a line, depending on the bodies' shapes (Figure 1). When external forces or displacements are applied, the two elastic bodies deform and therefore the contact zone becomes a definite contact area whose shape depends on the load magnitude. Hertz solved the elastic contact problem under the assumptions of a frictionless non-conforming contact between linear elastic bodies for which the contact area is small compared to the bodies' dimensions. Different geometries have been studied [9], here we will recall the particular case of contact between a cylinder and a half-plane.

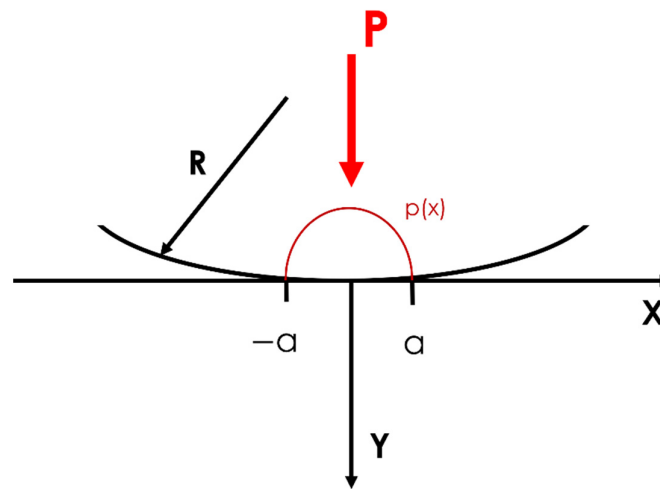


Figure 1. Contact configuration for Hertz theory, with normal contact pressure distribution.

The normal force P results in a contact patch of width $2a$ over which a pressure $p(x)$ is developed:

$$p(x) = p_0 \sqrt{1 - \left(\frac{x}{a}\right)^2} \quad (1)$$

where:

- $p_0 = \frac{2P}{\pi a}$
- $a^2 = \frac{8PR(1-\nu^2)}{\pi E}$

for the case of elastically similar bodies with Young's Modulus E and Poisson's Ratio.

In 1938, Cattaneo [10] extended the Hertzian contact problem to include the action of friction and consequentially tangential loads, therefore introducing interfacial partial slip. He first approached the problem considering the application of a constant normal load P and a monotonically increasing tangential load Q , starting from zero, to the three dimensional Hertzian case of elliptical contact area. The axisymmetric case of a fourth-order function was also treated later in 1947 ([11,12]). The same problems were treated

independently by Mindlin firstly in 1949 [13], while new generalizations on the loading path were later considered ([14,15]). In these cases, the normal pressure distribution remains unchanged, but shear tractions are developed to sustain the tangential force. A central stick zone $|x| < c$ is formed, bordered by two slip zones in which limiting friction acts (Figure 2).

The shear tractions $q(x)$ are given by:

$$q(x) = \mu p_0 \sqrt{1 - \left(\frac{x}{a}\right)^2} + q'(x) \quad (2)$$

where:

- $q'(x) = 0$ if $a > |x| > c$
- $q'(x) = -\mu p_0 \frac{c}{a} \sqrt{1 - \left(\frac{x}{c}\right)^2}$ if $|x| < c$

The size of the stick zone c is revealed by enforcing tangential equilibrium:

$$\frac{c}{a} = \sqrt{1 - \left(\frac{Q}{\mu P}\right)} \quad (3)$$

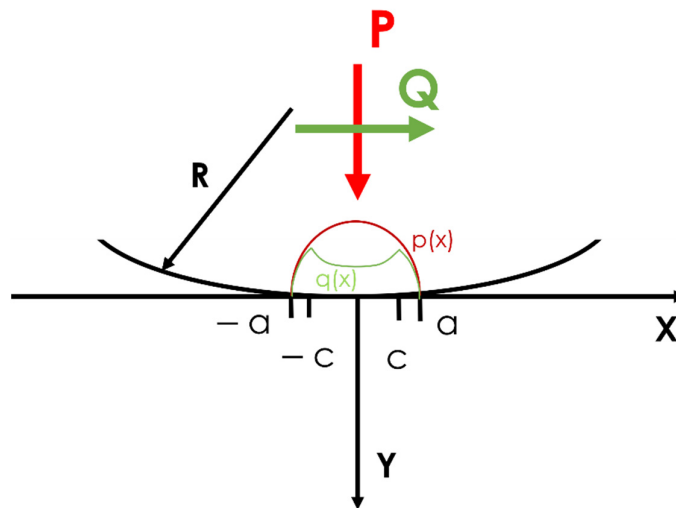


Figure 2. Contact configuration of the Cattaneo–Mindlin problem, with normal and tangential contact load distribution.

Introducing the cyclic nature of force Q , Mindlin and Desesciewicz [15] concluded that the resulting shear stress distribution is cyclic between limiting values of $\pm q(x)$.

In the late 1990s, Ciavarella extended the Cattaneo–Mindlin problem to more geometries [16], being able to exactly solve the 2D contacts problem but only approximating the solution for three dimensional contacts.

The Cattaneo–Mindlin configuration has been frequently adopted as the setup for fretting fatigue experimental testing. However, it must be highlighted that the presence of bulk stress during the experimental tests made tangential load distribution differ from the Cattaneo–Mindlin solution. Many years later, in 1987, Nowell and Hills analytically studied the effect of bulk tension on the stress distributions for the Cattaneo–Mindlin case [17]. It was demonstrated that the bulk stresses in the specimen introduced an eccentricity to the contact stick zone due to strain mismatch (Figure 3).

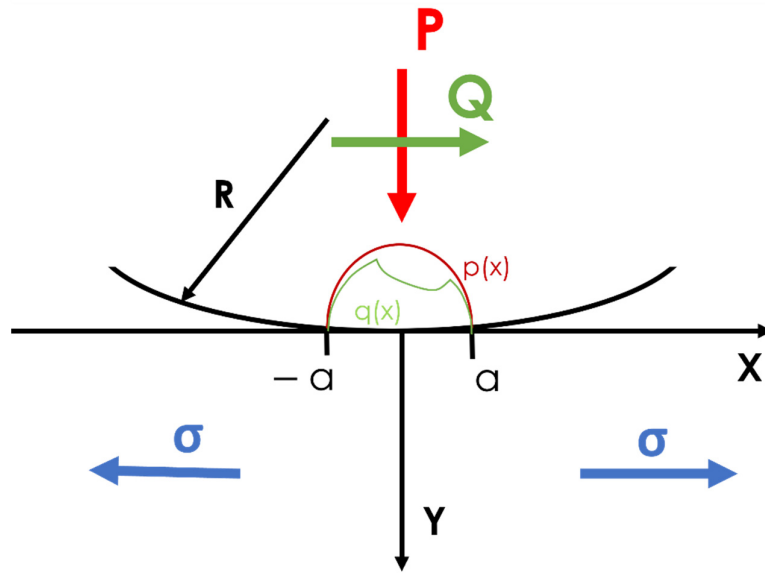


Figure 3. Contact configuration for Nowell–Hills solution with normal and tangential contact load distribution.

Barber et al. [7] applied periodic tangential loads and periodic normal loads to Ciavarella’s case. The contact problem was studied considering $Q = \mu P$ so that gross slip would not occur. They concluded that the extent of the permanent stick zone during steady state was independent of the loading path while the interior traction distributions depended on it.

1.2. Fretting Damage in Structural Joints

Understanding the fundamentals of fretting fatigue and fretting contact is crucial not only from the scientific point of view, but also from the practical point of view since there have been numerous reports of failures involving a wide variety of common structural members [18–27] due to fretting damage. Press fitted joints, dovetail joints and bolted joints have been reported to be strongly affected by fretting fatigue, since they operate under quite high normal contact loads and vibrations during service, which triggers relative displacement. Many studies are already present in literature, all concerning experimental tests, development of new test fixtures, analytical studies, or numerical studies on these joints (Figure 4). Therefore, the aim of the next sections is to give an insight of these literature studies that have been carried out, following chronological order, highlighting the most relevant results and the steps made throughout the past 60 years.

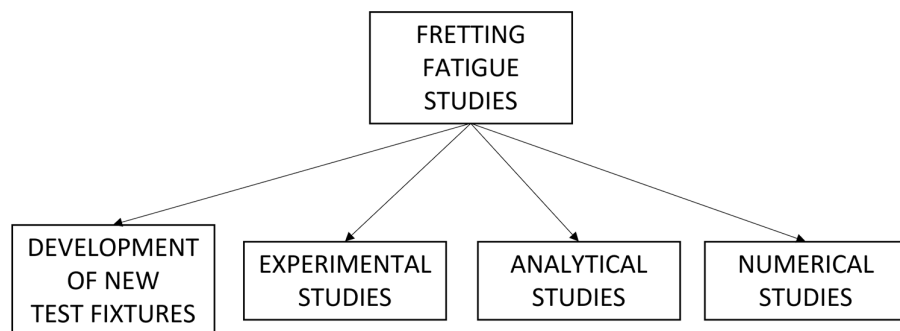


Figure 4. Scientific studies categories.

2. Press Fitted Shaft-Hub Joints

The press-fitted shaft-hub joint is a commonly used method to assemble mechanical parts. The retaining capability of such joints is proportional to the coupling pressure developed at the interface between the shaft and the hub by the radial interference between the members. This type of joint implies a certain amount of radial deformation of the shaft which acts exactly like any other geometrical discontinuity, subjecting the area to a local stress peak and therefore, with the presence of external time dependant loads, to fatigue failures. Practical examples of interference-fitted joints might be railway axles, the front forks of bikes or motorbikes, and turbogenerator rotors. The occurrence of fretting increases the need for finding a method to safely design this kind of joint even more, since it has been reported [28,29] that fretting crack nucleation happens for loads below the fatigue limit of the material.

The first series of tests with a cylindrical contact involved was undertaken in the late 1960s by Nishioka and Hirakawa [3,30–35]; this set of studies was also the first comprehensive series of studies about fretting fatigue in general.

Firstly, they tested different shape shaft specimens on a rotating-bending machine in order to replicate a classical fretting situation. They used a special sensor (Figure 5b) in order to measure the relative displacement occurring at the interface between the shaft and hub when subjected to the bending moment.

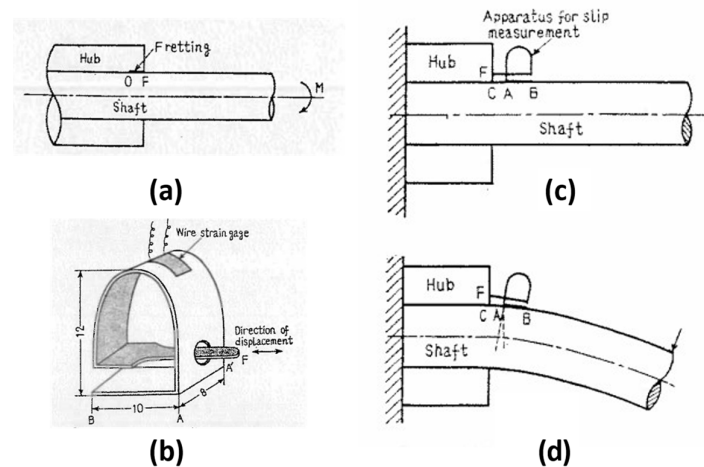


Figure 5. Schematics of the fretting fatigue test: (a) schematics of the load applied to the shaft-hub coupling; (b) relative slip measurement sensor; (c) schematics of the shaft-hub and sensor assembly before and (d) after applying the load [30].

In the first paper of the series [30], the existence of non-propagating fretting fatigue cracks is reported, suggesting that, although fretting may initiate and cause the initial growth of cracks, there may be combinations of parameters under which these cracks self-arrest. Another conclusion reached is that the amount of relative slip between the surfaces had an effect on the fatigue life. Further investigations [3,31] carried out by means of a new fretting fatigue fixture (Figure 6) made determination of the initiation site and direction of initial propagation possible. Cracks were found to start in a high stress region, next to the edge of the contact, and to propagate obliquely under the contact during the initial phase of growth. Another interesting observation was the increase in the coefficient of friction during the experiment from 0.2 to 0.67, with the maximum reached after 100 cycles.

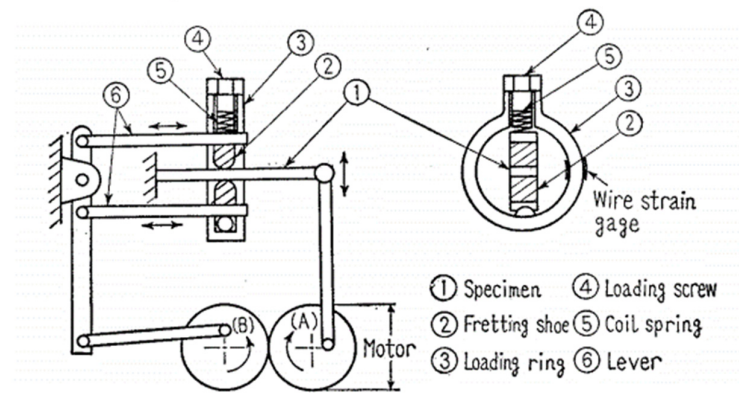


Figure 6. Fretting fatigue testing machine [31].

The effect of the mean value of the alternating stress applied to the specimen on the fatigue life in fretting was also investigated [32]. They found that it had little effect on the initiation of cracks, but that a higher mean stress in the specimen reduced the fatigue life. Hence, fretting was seen to be a central factor in the formation of micro-cracks. The independence of this process from the alternating bulk stress within the specimen suggests that it was controlled by local stresses at the contact. The bulk stress played a significant role in the later stages of propagation just as in normal fatigue. The effect of slip amplitude was further investigated in the fifth paper [35] where they first demonstrated that, if a tangential force less than that necessary to cause sliding was applied, zones of micro-slip developed at both edges of contact. Furthermore, in this regime of partial slip, the tangential force and the amount of slip were dependent variables, so that a greater tangential force caused larger amounts of slip. The fatigue life was dependent on slip, but this effect could be explained purely in terms of the higher tangential force required and the consequent increase in local stresses. At very large values of slip, where full sliding took place, significant wear was again reported. In the sixth paper [33], Nishioka and Hirakawa investigated the effect of material hardness and of contact pressure. Hardness was found to have little effect on the fretting fatigue life, while increased contact pressure resulted in reduced life, but since their experiments were run at a constant slip amplitude, the increase in contact pressure simply allowed a higher tangential force to be sustained in full sliding and this was thought to be responsible for the reduction in life. In the latest work [34], they tried to improve the rotating bending fatigue strength of press-fitted assemblies by means of geometrical variations of the press-fitted portion. They ran a series of experiments on the rotating-bending machine, investigating the behaviour of five different specimens, shown in Figure 7. The type D specimen displayed the maximum increase in the fatigue limit. However, it was observed that the type B specimen had a 50% longer fatigue life than the type A specimen, and from previous work [30], the type C specimen was found to have a longer fatigue life than type A. The type E specimen was found to have the longest fatigue life when considering the reduction in fretting corrosion, as confirmed in later works [36,37].

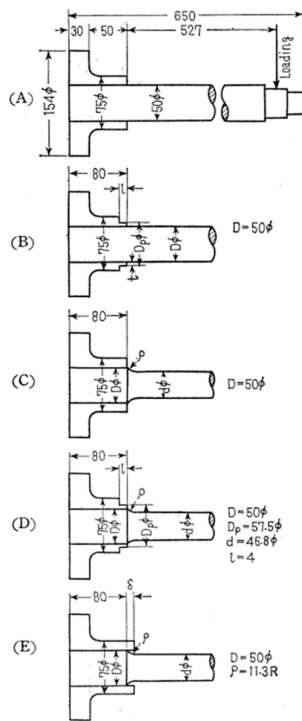


Figure 7. (A) Type A, (B) type B, (C) Type C, (D) Type D and (E) Type E shaft-hub specimens used by Nishioka and Hirakawa [34].

In 1998, Hirakawa et al. [38] investigated various design expedients that could improve railway axles' fatigue life. In particular, they found that adding a stress relief groove in electric passenger car axles could improve the fatigue life of the axle by up to 50% (Figure 8). They concluded that, in order to ensure the safety of the railway maintenance, inspections of fatigue cracks were still of critical importance and more investigation had to be carried out.

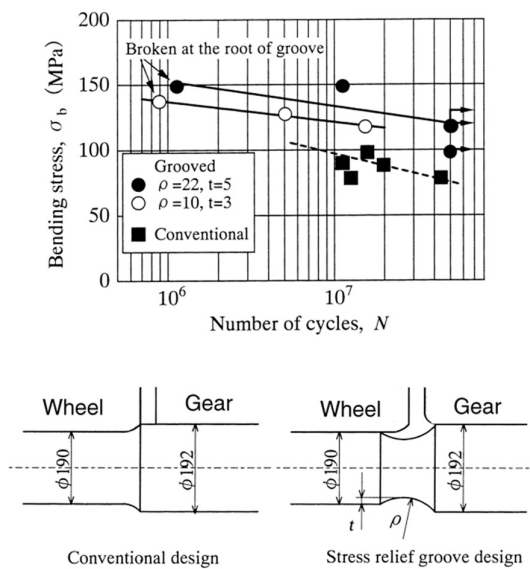


Figure 8. Effect of stress relief groove on fretting fatigue life of the axle. Reprinted with permission from Ref. [38]. Copyright 2022 Elsevier.

Another set of studies was carried out between 1999 and 2000 by Juuma [36,37]. He further investigated the effect of contact pressure, slip amplitude and geometry of the shaft and hub on the fretting fatigue limit of a S355J2 shaft-hub coupling. He divided the fatigue tests into two groups, for the first one, grooved hubs were used while, for the second one, plain hubs were used. A torsional vibration was applied to the two different types of specimen by means of the test rig showed in Figure 9.

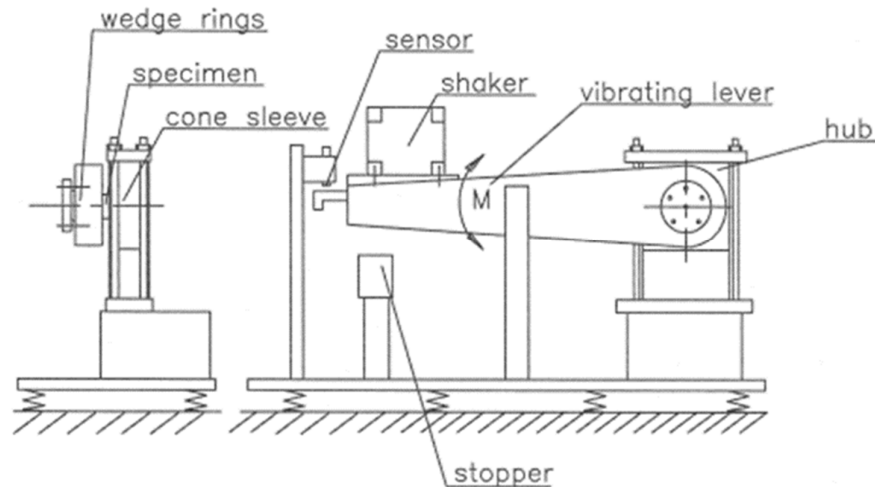
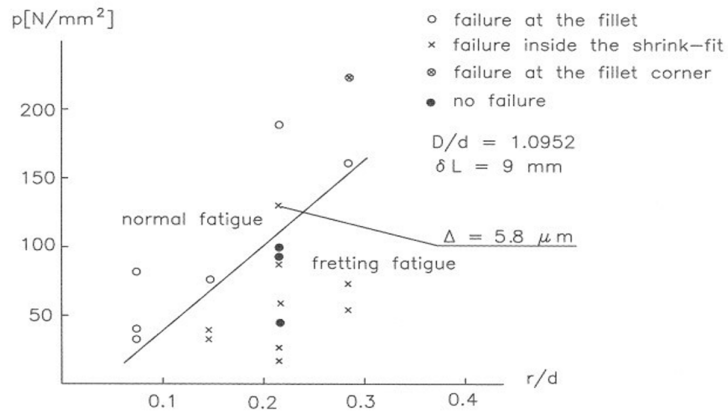


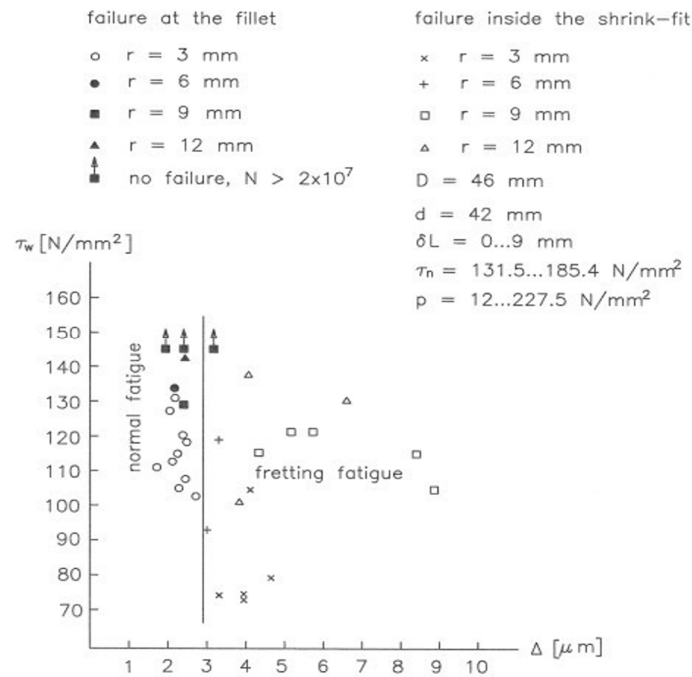
Figure 9. Schematic drawing of the test rig used by Juuma [36]. Reprinted with permission from Ref. [36]. Copyright 2022 Elsevier.

In general, it was found that fretting fatigue life increased with increasing contact pressure because slip amplitude decreased and therefore no fretting would occur. For the same reason, the hub overhanging the shoulder of the filleted shaft was confirmed to increase fretting fatigue life. However, it was also highlighted that, beyond a certain level of contact pressure, no more improvement in terms of slip amplitude was observed in grooved hub specimens, and that failure would then occur due to normal fatigue. Both normal and fretting fatigue life limits were found to increase with the increasing of the fillet radius until a certain value at a constant diameter ratio for grooved hub specimens. For radiuses above said limit, specimens were found to fail due to fretting. Some of the results are reported in Figure 10.

A few years later, Gutkin and Alfredsson [23] presented a study on crack growth prediction on shrink-fit assemblies subjected to rotating bending. In order to retrieve the initial crack size and the final crack size to be used and compared with numerical data, an experimental campaign was carried out on shrink-fit specimens (Figure 11a) made of Swedish standard 2140 steel (tool steel). A numerical simulation using FEM (Figure 11b) was then developed, in order to evaluate the contributions of the fretting contact on crack growth, the computed stress cycle was also required as an input to the numerical routine. Another FE model (Figure 11c) was used to compute the Stress Intensity Factor (SIF) along the crack in order to compare it with those retrieved using the Three-Parameter Procedure (TPP) developed by Nilsson [39]. Linear Elastic Fracture Mechanics (LEFM) was assumed to be valid since it was found that as long as the size of the plastic zone at the crack tip is small, LEFM could be applied [40,41]. The TPP numerical routine was found to be an efficient tool: the predicted crack growth life was found to be slightly less than 50% of the total fretting life in experiments, leaving enough space for crack initiation (Figure 12). The exact life decrease, however, depended on contact pressure and the coefficient of friction. In the studied conditions, an increase in contact pressure, or an increase in the coefficient of friction, resulted in shorter fatigue crack growth life.



(a)



(b)

Figure 10. Experimental results obtained: (a) effect of contact pressure and fillet radius and (b) effect of slip amplitude and fillet radius on fatigue failure with a grooved hub [36]. Reprinted with permission from Ref. [36]. Copyright 2022 Elsevier.

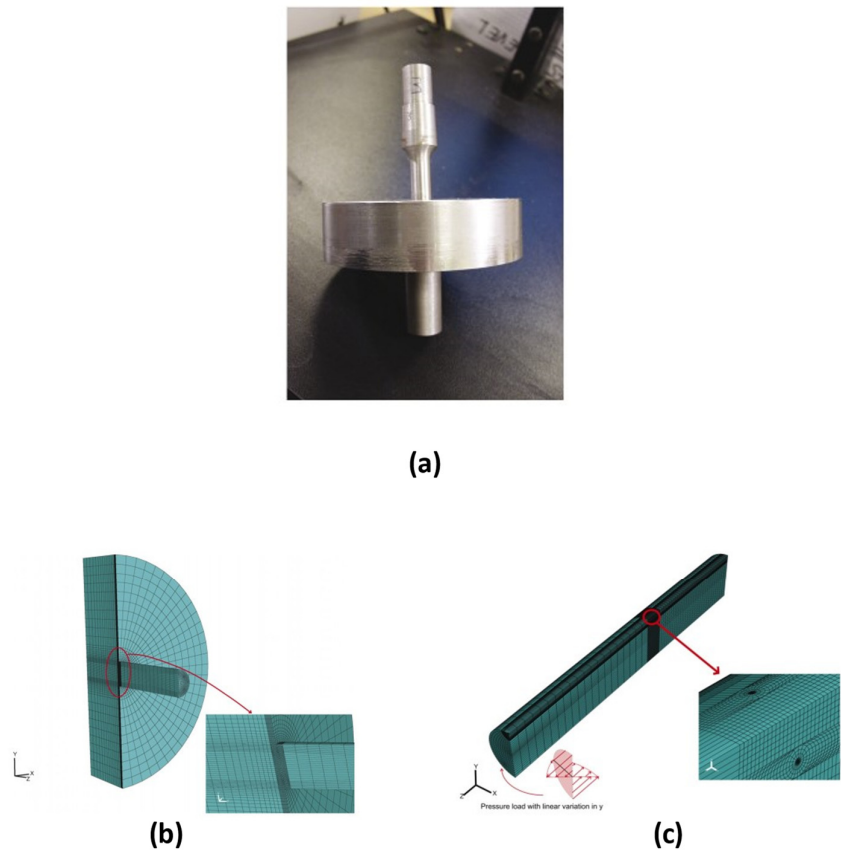


Figure 11. (a) Specimen, (b) general FEA model and (c) crack growth FEA model used by Gutkin and Alfredsson Reprinted with permission from Ref. [23]. Copyright 2022 Elsevier.

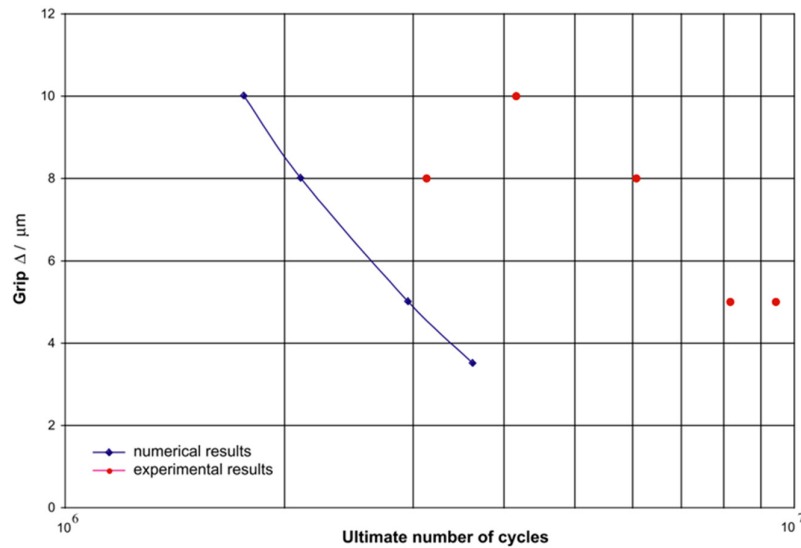


Figure 12. Radial press-fit grip-ultimate number of cycles. Experimental results include both crack initiation and propagation life, whereas the numerical results only contain crack propagation to failure Reprinted with permission from Ref. [23]. Copyright 2022 Elsevier.

Lanoue et al. [42,43] investigated the effect of different mesh sizes and contact algorithms (Pure Penalty function, Augmented Lagrange, Normal Lagrange and Pure

Lagrange were investigated) on the FE modeling of interference fitted assemblies. They replicated the type A specimen of Nishioka [35] (Figure 13). They observed that mesh refinement was a key point in achieving convergence, while all the contact algorithms that were used gave accurate results. Due improved computational efficiency, the authors recommended using the Augmented Lagrange algorithm.

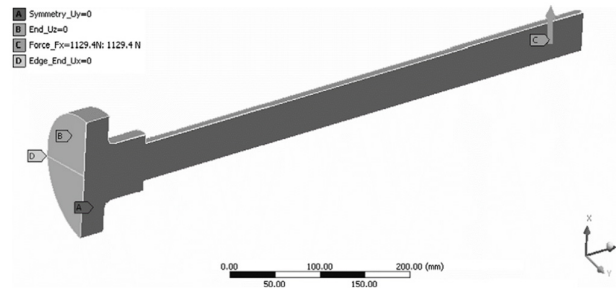


Figure 13. FE model used by Lanoue et al. [42]. Reprinted with permission from Ref. [42]. Copyright 2022 Elsevier.

During the last 10 years, other studies on railway axles have been carried out [25,44–46]. Linhart and Černý [44] investigated the behaviour of the axles made of different materials, specifically EA1N, EA4T and 34CrNiMo6 steel, in high-cycle fatigue conditions. These materials are considered to be standard materials for railway axles according to EN13261 and were also chosen for their very different strengths (from 586 MPa to 1041 MPa). Tests were carried out on a rotating bending machine using the shaft and hub specimens showed in Figure 14. Considering the fatigue limit evaluated at 5×10^7 cycles, if no failure occurred, or the depth of the fretting cracks, if initiated, was considerably less than 1 mm, the fatigue limit of EA1N and EA4T steel shafts was found to be in the range between 100 and 120 MPa, and between 85 and 105 MPa, respectively. The fatigue limit of 34CrNiMo6 steel shafts was found to be in the range of 95–105 MPa. In spite of considerable differences in strength and alloying of tested bars, differences in the mean value of the fatigue limit were not significant. Therefore, no significant increase in fatigue strength under press fit can be expected using a higher strength steel.

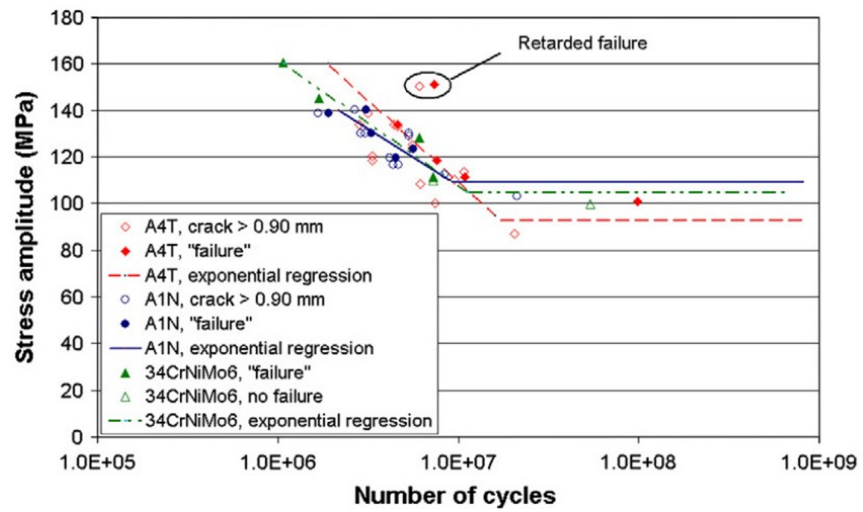
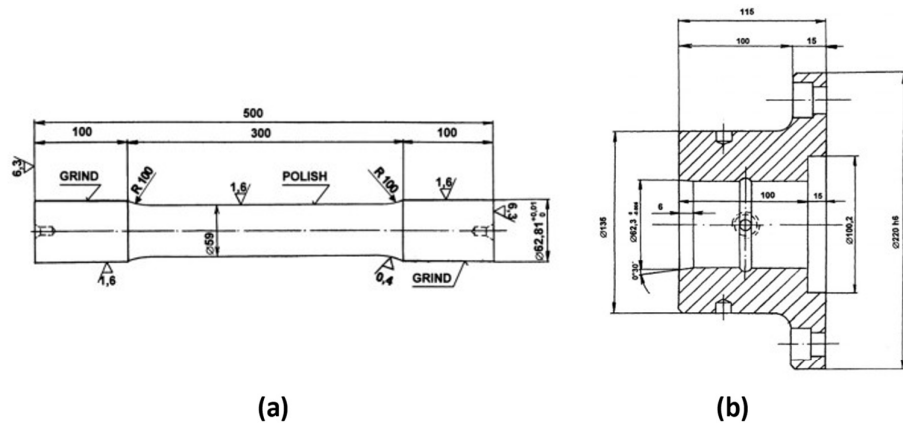


Figure 14. (a) Shaft and (b) hub specimens used by Linhart and Černý, with (c) comparison of the fatigue tests results [44]. Reprinted with permission from Ref. [44]. Copyright 2022 Elsevier.

Between 2013 and 2014, Croccolo et al. [47,48] designed an ad hoc shaft-hub notched specimen in order to study the fatigue behavior of this type of joints with a scaled test. The particular specimen fatigue behaviour was confronted with the plain fatigue specimen's ones. It was found that the fatigue behavior of the notched specimens was worse than the plain ones. The experimental fatigue stress concentration factor was therefore confronted with the one retrieved via FEA, and it was found to be significantly higher. This was explained with fretting fatigue concurring to crack initiation, and this hypothesis was confirmed with further metallurgical analysis [49]. At present, further work has been initiated, and the group is working on a new shaft-hub specimen (Figure 15) and analyzing the effect of fretting on the new specimen.

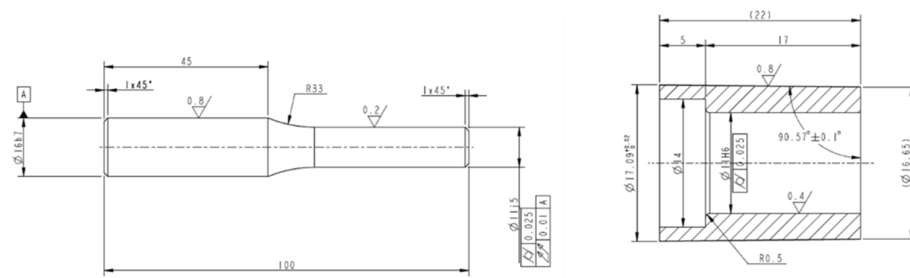


Figure 15. Evolution of the shaft-hub specimens designed by Croccolo et al. [48].

Song et al. [45] carried out a damage analysis on railway axles and ran small scale simulation tests on a rotating bending machine. The small specimens had a diameter of 10 mm. The materials tested were LZ50 for the axle and Class 60 for the wheel. Both are construction steels. The small-scale specimens’ behavior was in good agreement with the real axle ones. In both cases, the fretting fatigue crack initiated at the subsurface in correspondence to some inclusion cavities. The fretting cracks first propagated along an inclined angle controlled by the contact stresses, then they followed a somewhat radial path controlled by a combination of the contact stresses and the bulk fatigue stresses. It was, however, highlighted that a scale effect factor, even though hard to quantify without experimental parameters, should be considered for more accurate results.

Luke et al. [46] tried to give even more support to the development of a method that could be used to reduce the use of full-scale axle tests in favour of small-scale specimen tests. The schematics of the fixture used are showed in Figure 16, the tests were all run using EA4T steel for specimens and ER8 for the pads.

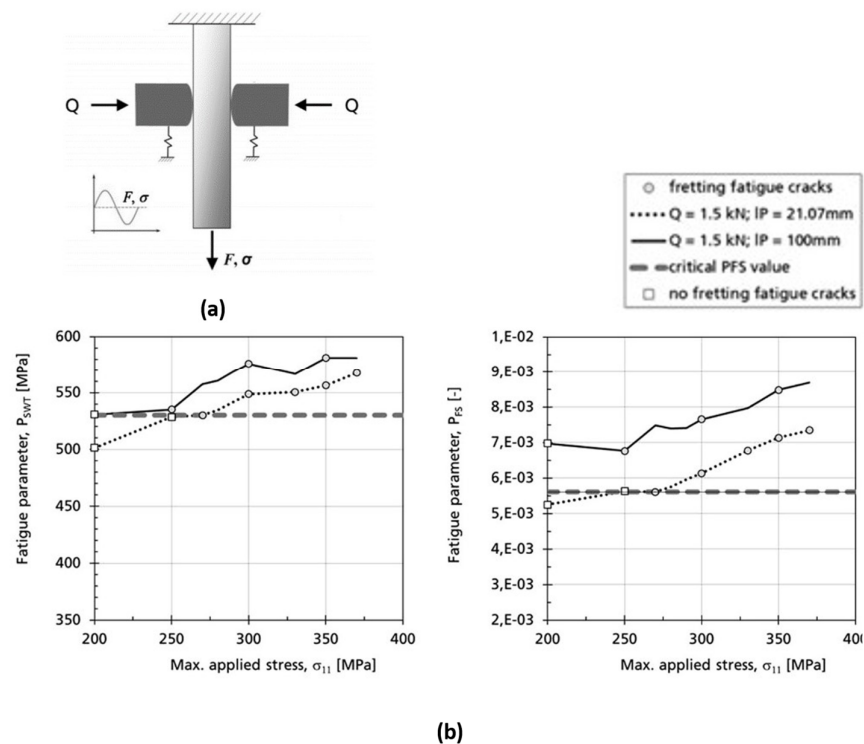


Figure 16. (a) Schematics of the fretting fatigue apparatus [49] and (b) comparison of the fatigue parameters SWT and FS for two different specimens Reprinted with permission from Ref. [46]. Copyright 2022 Elsevier.

The load parameters, such as the stress amplitude, contact load and relative slip between the contact surfaces, were varied or selected to achieve conditions relevant for axles in service. Two-dimensional numerical analyses reproducing the fretting fatigue tests were also run in order to evaluate the possibility of using the following multiaxial fatigue parameters to predict possible material damage under fretting fatigue conditions:

- $SWT = \sigma_{max} \cdot \varepsilon_a$, where σ_{max} is the maximum normal stress in one cycle on the critical plane and ε_a is the normal strain amplitude on the critical plane [50];
- $FS = \frac{\Delta\gamma}{2} \left(1 + \alpha \cdot \frac{\sigma_{max}}{\sigma_y} \right)$, where $\Delta\gamma$ is the maximum shear strain range, σ_{max} is the maximum normal stress in one cycle, σ_y is the yield stress and α can be approximated to 0.5 [51].

The experimental results demonstrated that increasing the contact area facilitated fretting fatigue crack initiation, as was also previously said by Hills et al. [52]. It was also confirmed that a larger contact slip brought a higher probability of crack initiation for equal nominal external load. Both multiaxial parameters turned out to be helpful in the quantitative assessment of crack initiation under fretting fatigue.

More recently, a set of studies about the influence of wear on fretting fatigue has been carried out by Zhang et al. [53–55]. In the first study [53], they ran a series of interrupted rotating-bending fatigue tests on press-fitted shaft specimens (Figure 17). A three-dimensional finite element model with fretted wear scars was developed in order to simulate the interrupted specimens. In this way, they were able to study the evolution of surface damage and its influence on fretting fatigue by means of the multiaxial fatigue parameters SWT [50] and FS [51] jointly with a critical plane approach. The main conclusion was that wear shifted the crack initiation location from the contact edge to the inner area, causing the initiation life to increase accordingly. Therefore, it is concluded that wear should be taken into account when using critical plane approaches such as SWT and FS .

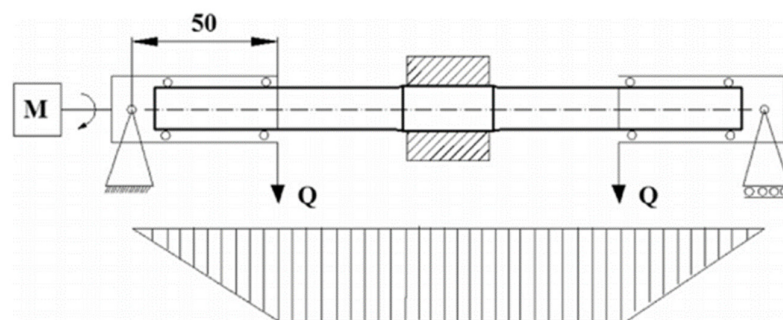


Figure 17. Schematics of the fretting fatigue apparatus. Reprinted with permission from Ref. [53]. Copyright 2022 Elsevier.

In [54], a finite element methodology that combined a wear model proposed by Fouvry et al. [56] and the critical plane SWT approach with a correction proposed by Ince et al. [57] was later proposed, since the classic SWT parameter could be non-conservative for cyclic loads involving large compressive mean stresses. It was concluded, as previously noted, that wear promoted the fretting crack initiation at the inner surface of the contact area because of large stress concentration near the fretted wear scar edge, whereas fretting wear significantly reduced fretting crack initiation at the contact edge by grinding off the surface material with fatigue damage, and by reducing the stress concentration there. In their latest work, [55], they applied the developed FE methodology on a press-fitted railway axle model (Figure 18), investigating in particular the influence of the stress relief groove. The numerical results were compared to experimental results

retrieved from the literature, finding good agreement concerning the crack initiation location. It was also found that either the increase in groove depth or the decrease in groove radius could reduce the fretting wear and improve the fretting fatigue strength through relieving the stress concentration. It must be underlined, however, that increasing the groove depth or decreasing the groove radius above a certain limit increases the chances of developing conventional fatigue cracks on the groove itself.

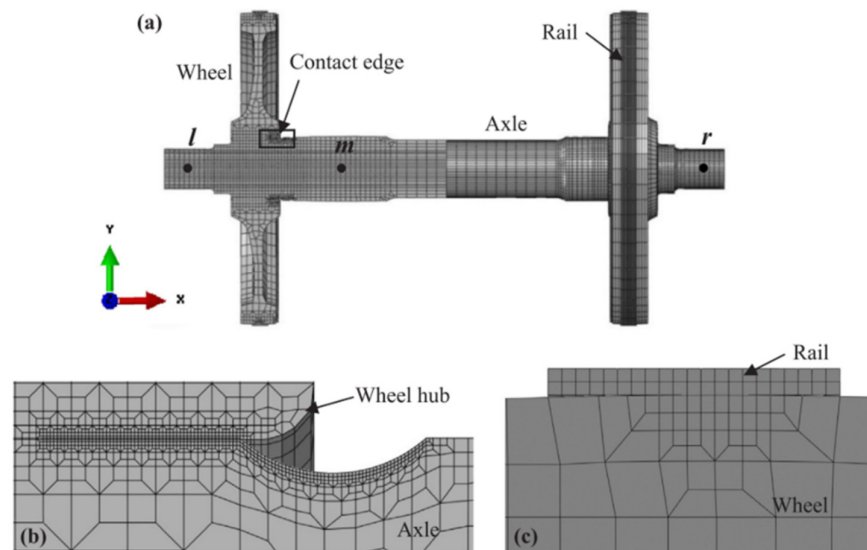


Figure 18. FE model used: (a) overview, (b) detail of the contact between wheel seat and wheel hub and (c) detail of the contact between wheel and rail [55]. Reprinted with permission from Ref. [55]. Copyright 2022 Elsevier.

Most Significant Results

To summarise, the most important results from the studies in this section are:

- In fretting conditions, cracks develop near the edge of the contact area, corresponding to the peak contact stress. However, if fretting wear occurs, cracks have been reported to initiate at the inner surface of contact area because of peak stresses occurring at the edge of the wear scar. At the same time, fretting crack initiation at the contact edge is significantly reduced because of the cracks getting ground off;
- A stress relief groove and, possibly, a hub overlap, increases fretting fatigue life. Mixed results have been reported about the influence of the groove radius. More experimental results are needed in order to define the benefits or disadvantages of increasing or decreasing the groove radius;
- It was reported that no significant increase in fatigue strength under press fitting can be expected for high strength steels;
- Use of fretting fatigue criteria such as the *SWT* and the *FS* criterion was found to be useful to identify the crack nucleation location. More research is needed in order to assess the use of these parameters;
- Linear elastic fracture mechanics (LEFM) and TPP numerical routine proved to be efficient tools for the evaluation of the crack growth life.

3. Dovetail Joints

Dovetail joints are widely used in the aircraft propulsion field as a means of connecting the blades and disks of rotating turbines and compressors. Fretting fatigue design is of primary importance in the fan assembly and in the low-pressure stages of the compressor where the operating temperature is low enough to exclude creep damage.

During the engine duty cycle, the contact area between the root of the blade and the disk experiences high levels of pressure and bulk stress while the two bodies are subjected to relative displacements, making it likely for the assembly to develop fretting fatigue damage.

A first set of specific studies and tests about fretting fatigue in dovetail joints has been carried out by Ruiz together with Boddington during the '80s [58–61]. They overcome the expensive and time-consuming spinning-disk tests by developing a new simple specimen consisting of a rectangular sheet modeling the disk, with three pair of blades jointed back-to-back to said sheet by means of dovetails, as shown in Figure 19 [58]. The specimen was loaded under biaxial tension in a fatigue testing machine in which two hydraulic actuators, acting on sheet and blades, respectively, were controlled to operate between any two independent loads, displacements or strains, in-phase or out-of-phase. The specimen was then tested [59] for a total of 28 tests, carried out for an applied load to the sheet in ranges of 2–20 kN, 4–40 kN and 4–80 kN. All specimens were crack detected by dye penetrants and photographed under UV light. The fatigue life corresponded to the instant when a crack became visible under the intense illumination of two 500 W lamps.

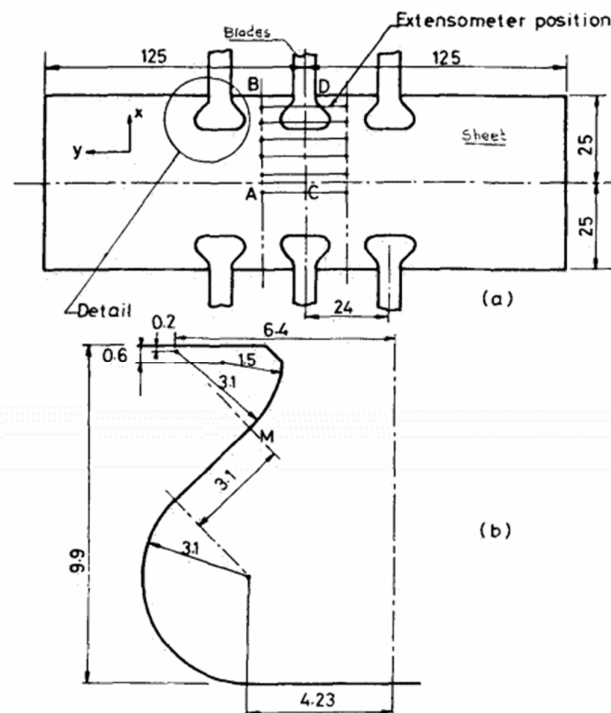


Figure 19. General arrangement of (a) test piece and (b) dovetail profile. Reprinted with permission from Ref. [59]. Copyright 2022 Springer Nature.

The materials tested were for the blades Fv 535 (X8CrCoNiMo10-6) and Incoloy 901 (NiFeCr12Mo), and for the sheet IMI 829 (Ti-6Al-4V) [62]. The results indicated that:

- Increasing the sheet loading increased the width, roughness and depth of the fretted region;
- For equal condition of loading and same material, fretting reduced fatigue life;
- For equal condition of loading and material, frequency did not affect the fretting phenomenon.

In the same work, numerical analysis of the joint was carried out using a code previously developed by Boddington et al. [61]. Since cracks were initiating away from

the point where the peak tangential stress occurred, they concluded that other parameters were to be considered, such as surface damage.

They consequently proposed a design parameter, “fretting damage” (FD), by multiplying the highest surface tangential stress with the maximum frictional work:

$$FD = (\sigma_T)_{max} \cdot (\tau \cdot \delta)_{max} \quad (4)$$

where σ_T is the highest surface tangential stress, $(\tau \cdot \delta)_{max}$ is the maximum frictional work, τ is the surface shear stress and δ is the relative slip. However, the parameter did not give any indication of the location of the crack. An alternative parameter was proposed:

$$FFD = \sigma_T \cdot \tau \cdot \delta \quad (5)$$

This “fretting fatigue damage” (FFD) parameter reached its peak value next to the crack location regardless of loading. It was later reported, however, to predict the location of the crack but not to predict the number of cycles to crack initiation or crack growth [50]. Both the parameters are measured in $\frac{N^2}{m^3}$.

A single pair of back-to-back specimens was later tested and showed to provide satisfactory results [62].

Further experimental and numerical tests were run on dovetail geometry in 1994 by Papanikos and Meguid [63]. They compared different criteria to predict the direction of fatigue crack growth, concluding that the maximum–minimum principal stress criterion (MPS) [64] could reliably predict the general direction of the propagating cracks. Furthermore, they concluded that the crack growth rate under mixed-mode loading appeared to be rather lower than mode I loading.

A new testing rig was later designed by Hutson et al. [65] in 1999. In order to maximally simplify the geometries involved, they assumed that the bending moment induced by the dovetail geometry had no effect on the relative motion responsible for fretting fatigue damage. The test rig was composed of flat fretting pads, with a radius at the edge of contact, pressed against a flat specimen. The imposed normal and internal shear loads were reproduced in the test apparatus, as shown in Figure 20. The entire load applied to the specimen was transferred to the fixture by means of the fretting pads thus making the portion of the specimen beyond the contact area not subjected to bulk cyclic load.

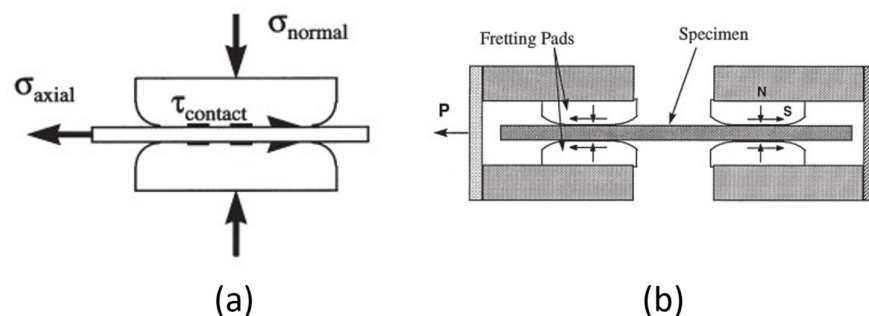


Figure 20. (a) Representation of test configuration designed to simulate blade root loading condition and (b) Test load train schematic. Reprinted with permission from Ref. [65]. Copyright 2022 Elsevier.

They tested Ti-6Al-4V specimens, retrieving the fatigue stresses defined by the maximum stress corresponding to a constant life of 10^7 cycles and analyzing fracture surfaces of the failed specimens using SEM. They found that the apparatus successfully reproduced the fretting fatigue condition and that all the failures occurred near the edge of the contact.

Around the same period of time, Ciavarella and Demelio analysed the problem of a flat rounded contact which represents more accurately the case of the dovetail joint. They first gave analytical results for surface traction and interior stress field in dependence of the geometry of the rounded edges, as shown in Figure 21. They found that if the contact transmits tangential loads, the concentration of tensile stresses at the trailing edge of a sliding contact is shown to always be significantly higher than the flat-on-flat case, but the transition to the infinitely high stress concentration associated with a sharp-cornered flat punch was slow (Figure 22) [66].

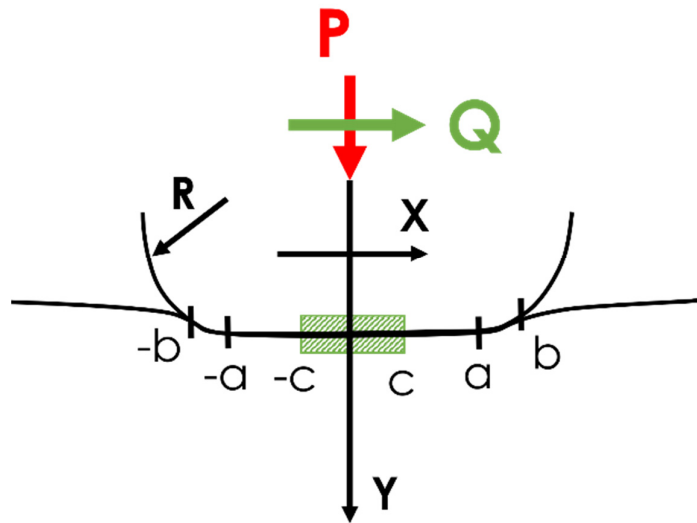


Figure 21. Geometry of the indenter. $2a$ is the length of the straight part of the punch, $2b$ is the contact length [66].

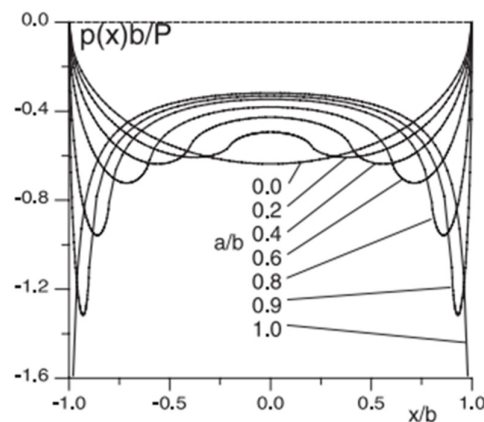


Figure 22. The contact problem for the radiused flat contact geometry (symmetrical contact): pressure distribution. Reprinted with permission from Ref. [67]. Copyright 2022 Elsevier.

They later tried to apply the analytical results to the evaluation of damage parameters [67]. They say that the *FFD* parameter, previously introduced by Ruiz [59], may not work for quantitative analysis, since it does not have a direct physical interpretation and since it is a hybrid approach which measures two competing processes by multiplying them arbitrarily with the same weight and at the same point. So, they focused on two other damage parameters: the slip amplitude δ and the frictional energy dissipation parameter D .

In particular, they found that under incipient full sliding, the following relationship is valid:

$$\delta_{max} = f \cdot g_{max} \quad (6)$$

where f is the friction coefficient and g_{max} is the maximum gap of the unloaded profiles. Together with these results, they provided the analytical formulas in order to retrieve the contact area, therefore providing a simple mean to compare different geometries. They also provided the extension for the evaluation of frictional damage:

$$D_{max} = f[p(x) \cdot g(x)]_{max} \quad (7)$$

where $p(x)$ is the pressure distribution and $g(x)$ is the gap function. Frictional damage is shown to have a weak dependence on geometry. The extended formula of the energy damage is:

$$D = D_0 \cdot \left(\frac{c}{b}\right)^2 \cdot \left[x\sqrt{x^2 - 1} - \log\left(x + \sqrt{x^2 - 1}\right)\right] \cdot \sqrt{1 - x^2} \left(\frac{c}{b}\right)^2 \quad (8)$$

where they introduced the normalizing parameter $D_0 = \frac{8}{\pi} \cdot (f \cdot p_m)^2 \cdot \frac{A}{\pi} \cdot b$ which highlights the fact that the friction coefficient and the average pressure extremely affect fretting damage. D_0 only depends on friction, contact pressure and general geometry of the indenter, making it easy to compare the damage produced for different contact locations.

They also pointed out how, based on their model, a smaller punch radius is expected to improve the fretting fatigue behavior, however, more studies were needed in order to define whether the benefit still holds true for a vanishing small radius.

In 2002 [68], they further revised the contact problem of the flat rounded punch using and developing the analytical results given by Ciavarella et al. [66]. A formula has been devised for estimating the peak value of the tangential stress σ_{bulk} :

$$\sigma_{xx}(b, 0) = 2 \cdot f \cdot p_{max} \cdot k \left[\sqrt{\left(1 + \frac{\sigma_{bulk}}{4 \cdot f \cdot p_{max}}\right)^2 - \left(1 - \frac{|Q|}{f \cdot P}\right) - \frac{\sigma_{bulk}}{d \cdot f \cdot p_{max}}} \right] + \sigma_{bulk}^P + \sigma_{xx}^P \quad (9)$$

The formula holds true for Hertzian geometry and moderate bulk, whereas it is approximate for either non-Hertzian geometry or large bulk, but the error is limited to within a few percent except in extreme cases (very flat geometries, low $\frac{Q}{f \cdot P}$ and large bulk stresses).

In 2003, Fridrici et al. [69] conducted a series of experiments to determine the influence in terms of fretting damage of a Cu-Ni-In coating on Ti-6Al-4V, due to the poor tribological behavior of the titanium alloy used for fan blades. Schematics of the used rig are shown in Figure 23.

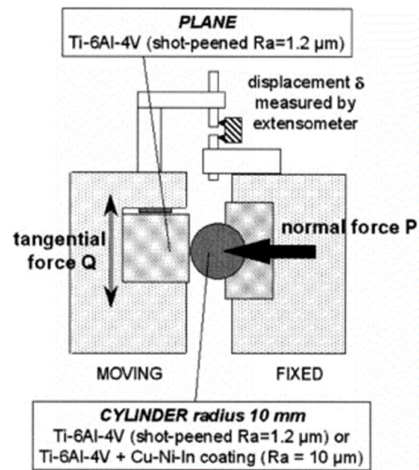


Figure 23. Schematic drawing of fretting-wear rig used by Fridrici et al. [69]. Reprinted with permission from Ref. [69]. Copyright 2022 Elsevier.

They mainly investigated the behavior of the coating in a fretting wear regime, but they found that the Cu-Ni-In coating reduced the length of the cracks observed on the counterbody in Ti-6Al-4V and that for different normal forces, the sliding amplitude could be taken as a unique experimental parameter to determine the domain in which cracks initiated.

In 2004, Conner et al. [70] tried to estimate the fretting fatigue life of several contact geometries, including a dovetail joint geometry, by using the crack analogue model [71]. Reasonable agreement was found between experiments and predicted life (Figure 24). It was pointed out, however, that the state of the material ahead of the crack or at the contact surface was different to the actual contact body and the crack analogue model body. Although it has been shown that the stress fields near the crack were identical, the fretting model did not show microstructural damage that would have developed in the real crack case. Therefore, a valid application of the model requires confirmation of conditions of small scale yielding in the contact region of interest. In particular, for more complex contact geometries, such as dovetail joints, it is necessary to determine point or line contact loads by numerical methods.

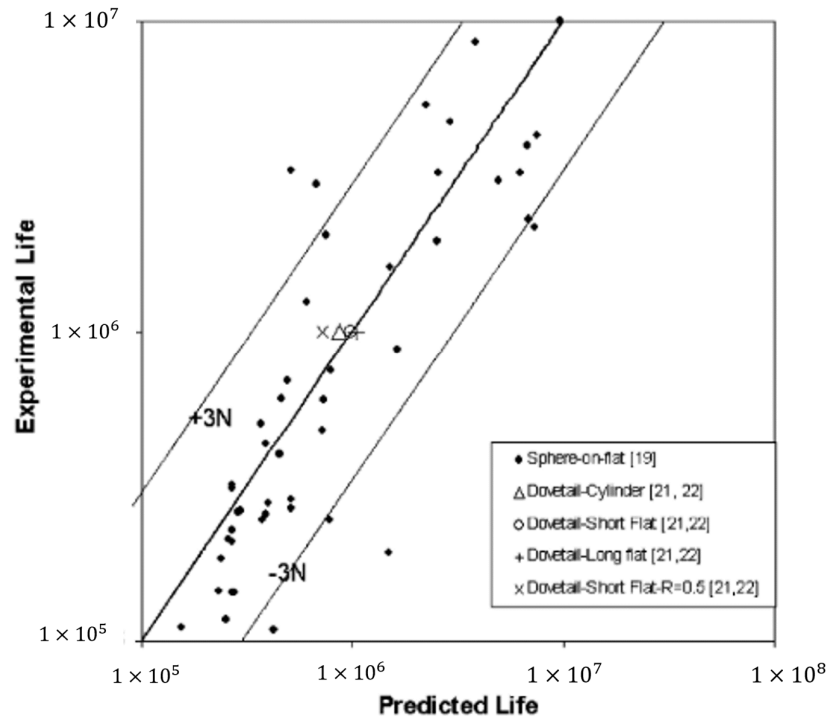


Figure 24. Comparison between experimental life and predicted life using the fracture mechanics method from Conner et al. [70]. Reprinted with permission from Ref. [70]. Copyright 2022 Elsevier.

They later developed a dovetail fixture (Figure 25) [72] so that cyclic, normal and tangential loads could be applied to the specimen. They tested several specimens in combination with several contact pads and different loads. They found that the short flat pad required the least load at a load ratio $R = 0.1$ to cause failure at 10^6 cycles.

They found that the application of the coating provided resistance to fretting fatigue crack initiation, probably because of the reduction in the coefficient of friction, and therefore reducing contact stresses. It resulted in an increase of nearly 25% of the baseline $R = 0.1$ loads to cause failure at 10^6 cycles.

Low plasticity burnishing was also shown to mitigate fretting fatigue damage, due to the compressive residual stresses which inhibit the nucleation of a crack or slow down the growth of fretting fatigue cracks by reducing the opening stresses during the fatigue cycle. In this case, an increase of 50% of the baseline $R = 0.1$ loads is required to propagate cracks to failure at 10^6 cycles.

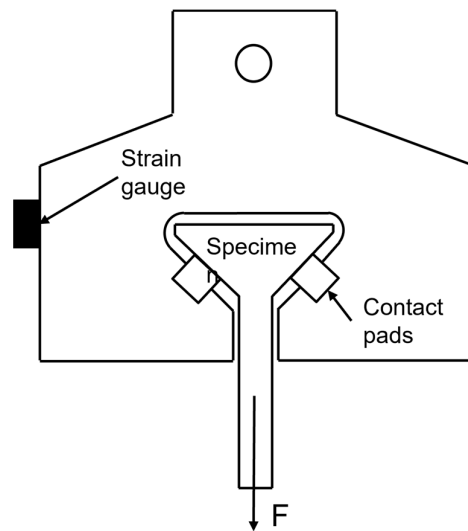


Figure 25. A schematic drawing of the dovetail fixture developed by Conner and Nicholas [73].

Meanwhile, in 2004, Murthy et al. [73] again approached the problem of pressure distribution evaluation in a contact between two generic surfaces using the single integral equations (SIE) already solved by Ciavarella. They further demonstrated the capability of the analytical model to analyze complicated load histories by testing it using a sample load history. They also evaluated subsurface stresses using this approach, successfully predicting the failure lives of fretting fatigue specimens.

A set of studies on dovetail joints was conducted between 2005 and 2009 at the Air Force Research Laboratory of Wright-Patterson, Ohio, USA. They tried to correlate contact stresses with the contact surface damage by developing a hybrid analytical and numerical process, supporting it with experimental results. They first ran experimental tests on a testing rig similar to the one developed by Conner and Nicholas [72] (Figure 25), using three different dovetail specimen geometries with different angles in order to investigate the effect of the angle on the fretting fatigue results. They still assumed that the dovetail was symmetric, and that the moment was negligible. They observed that for low R ($R = 0.1$), the specimen experienced gross slip for several thousand cycles until the average coefficient of friction increased. For higher R ($R = 0.5$) there was no initial gross slip. The test results showed little difference in terms of fatigue life between the three different angles, even though quite different contact loads were retrieved for the same remote load and life [74].

They then performed a finite element analysis of the dovetail fixture. Both coarse and refined meshes were used in order to capture the stress peaks at the edge of contact as accurately as practical. The singular integral equation (SIE) method was then applied using the output of the coarse finite element mesh and compared to results obtained using the fine mesh. They also analysed each of the two components using FEM in order to retrieve contact stresses. The results from these analyses were then used as inputs for the SIE method to determine the stresses at the contact edge. Such stresses were then used to determine the SWT [50] parameter, and the results were compared to a microscopic examination of the wear surfaces.

They observed the following:

1. a rough correlation between the SWT parameter and contact damage appeared to exist;
2. contact stress values appeared to be strongly dependent on the coefficient of friction;
3. the stress gradient died out at approximately the same depth for all gradients. This is significant because if this occurs for a wide range of geometries and frictional values, the bulk contact stress can be used to determine the likelihood of crack growth, given that contact stresses will initiate a crack to that depth [75].

In a subsequent work, they applied fracture mechanics life prediction methodology to evaluate its capability for predicting the performance of dovetail joints, by comparison again with experimental results [76]. They firstly used the same hybrid approach from the previous work to predict contact loads and bulk stresses, while the local contact stresses were evaluated for each SIE (singular integral equation) with the software CAPRI [73], as it was less time consuming than using a converged FEM solution for each case. It was found that the fracture mechanics crack growth predictions performed very well on this set of experiments (Figure 26). Furthermore, it was demonstrated that the potential exists for a crack to grow and arrest under fretting conditions due to a decreasing crack growth rate as the crack grows out of the local contact stress field. Finally, it was also demonstrated that the choice of initial crack depth, up to 100 μm , had little effect on life predictions due to the high initial crack growth rates.

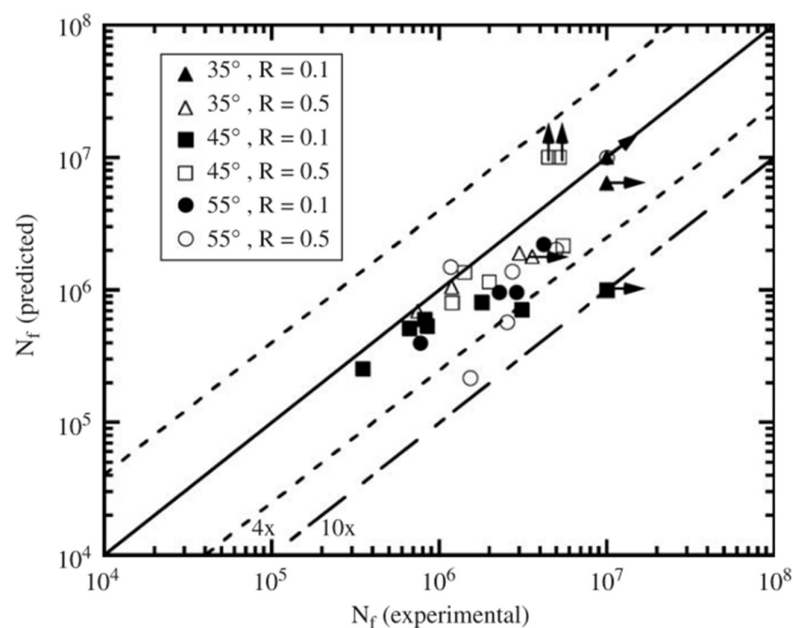


Figure 26. Comparison of experimental fatigue lives and predicted total lives [76]. Reprinted with permission from Ref. [76]. Copyright 2022 Elsevier.

They then tested various palliatives applied to Ti-6Al-4V specimens in order to determine their contribution to improving fretting fatigue life, as already studied by Conner and Nicholas [72]. In agreement with the previous work, they observed that low friction coatings such as Diamond Like Carbon (DLC) increased the number of cycles needed to nucleate a crack by reducing the magnitude of the applied loading, whereas surface processing inducing compressive residual stresses (low plasticity burnishing—LPB and laser shock processing—LSP) reduced the intensity factor range resulting in either retarded crack growth or crack arrest. In spite of that, they also found that these surface treatments did not eliminate the nucleation of fretting cracks, and also that a conjunctive use of both types of palliatives brought longer life to the specimen than the one without palliatives but with a very reduced life length compared to the only DLC or only LPB/LSP specimens (Figure 27) [77]. Thus, it is not recommended to use both palliatives.

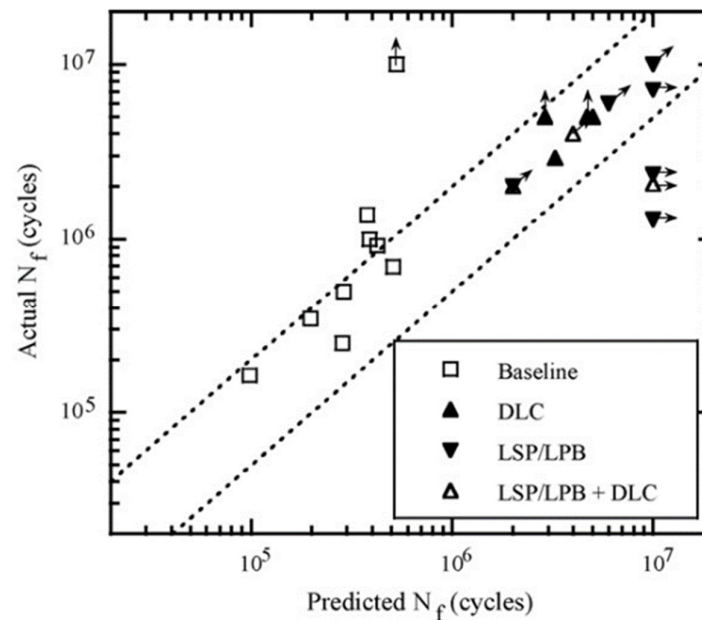


Figure 27. Comparison of experimental fatigue lives and predicted total lives of coated specimens [77]. Reprinted with permission from Ref. [77]. Copyright 2022 Elsevier.

They also run a set of experiments on Ti-6Al-4V specimens using three different fixtures already used in previous investigations, here called fixture A [65], B [78] and C [72]. Fixture A (Figure 28a) was used more appropriately to test longer contact lengths, while fixture B (Figure 28b) and C (Figure 28c) were used to reproduce contact regions with shorter flat lengths and cylindrical pad geometries. No gross slip occurred in fixture A tests: this is noticeable because the presence of wear damage might hide the presence of other damage mechanisms. In fixtures A and B, a step-loading procedure was performed for the tests: a certain known value of bulk stress was first selected so that the specimen would undergo a chosen number of cycles without fracturing. Then the bulk stress was increased by a small percentage and the block of cycles repeated. The process was repeated until fracture occurred and the fatigue limit strength could be interpolated. This step-loading procedure was not applied to fixture C tests, but the stress-life fatigue lives results were similar to those selected for fixture A and B tests. In order to evaluate the stress fields for the different loading conditions, finite element and numerical contact mechanics analyses run with software CAPRI were used, whereas fracture mechanics and a stress-life approach were used to assess the experimental results. It was found that fixture A and B results for the fretting fatigue limit correlated well with the stress-life parameter, explainable with the use of thin specimens compared to contact size and the presence of higher subsurface stress. For similar total lives in the range of 10^6 to 10^7 cycles, the stress intensity factor fields were shown to be different for each fixture; it was suggested to compute the fracture mechanics driving force for each fixture and to compare it with the stress intensity factor field threshold. In particular, fixture A and B were found to produce stress conditions where any crack that nucleated would continue to propagate and were, therefore, loads that could be related to a criterion for crack nucleation. Fixture C instead showed a stress intensity factor field that allowed for cracks to nucleate and arrest until the load required to exceed the long crack growth threshold was surpassed. Thus, the load causing failure in this case related to the threshold stress intensity factor range and not to a nucleation criterion. It can be concluded that the comparison between three fixtures highlights that a simple fracture mechanics model is not sufficient to explain all the experimental results [79].

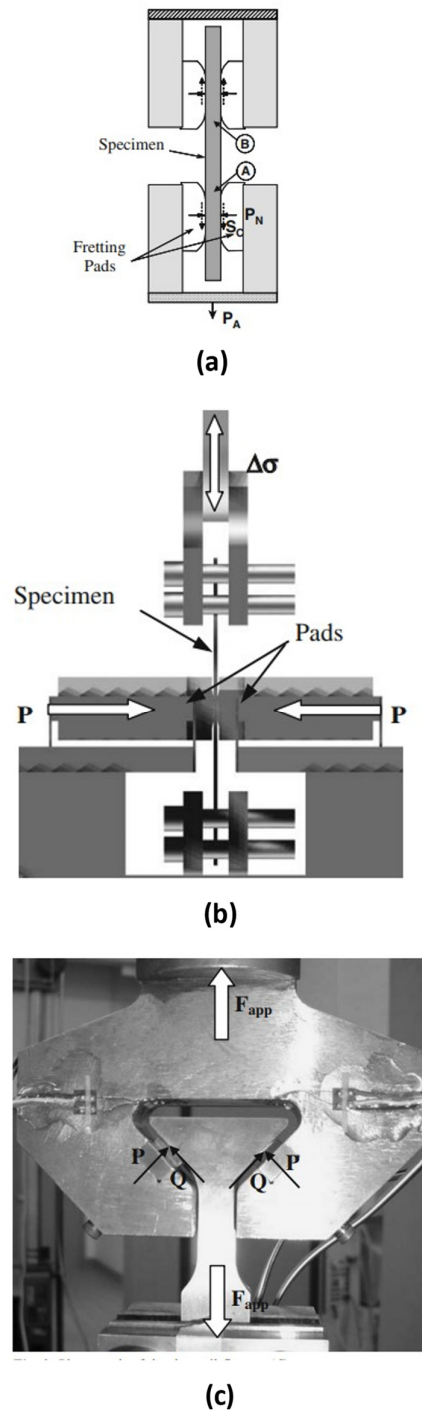


Figure 28. Dovetail fixtures: A (a) B (b) and C (c) [79]. Reprinted with permission from Ref. [79]. Copyright 2022 Springer Nature.

Lastly, they tried to develop a new fixture (Figure 29) for fretting fatigue testing at high temperatures. The new fixture was based on the previously used dovetail fixture, with the addition of:

1. two load cells in order to be able to directly measure the contact forces applied to the specimen;

2. the heating elements capable of simulating the temperature conditions in the attachment region of the turbine rotor.

They tested specimens made of nickel-based superalloy René 88DT while the fretting pads were made of crystal nickel-based alloy René N5. They found that the contact force measurement was dependent on a parameter that has not been fully validated yet. They also found a strong dependence on the symmetry of the system that can be adjusted by means of a set of screws, and measured by means of the load cells, but the influence of it on the contact force calculations has also not been validated. They concluded, however, that it could be observed that the specimens failed at the expected location and that fretting scars appeared as expected. Moreover, they validated the use of the temperature system, as it effectively controlled the temperature of the specimen. Further testing is needed in order to study the sources of variability [80].

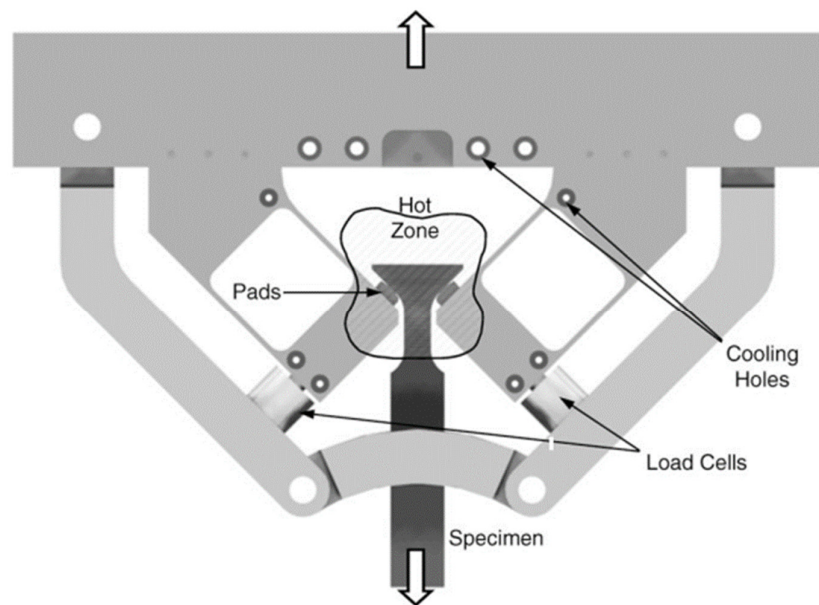


Figure 29. Schematic drawing of the high temperature dovetail fretting fatigue fixture [80]. Reprinted with permission from Ref. [80]. Copyright 2022 Elsevier.

In 2011, Anandavel and Prakash [81] studied the influence of three-dimensional loading and of the skew angle in a dovetail joint by means of a FE three dimensional model. The geometries considered are shown in Figure 30. The loads considered are shown in Figure 31, in particular, they considered the centrifugal force F_{mr} (constant when the blade is rotating at constant angular velocity), the aerodynamic force F_p (resulting in axial and tangential force components, cyclic in nature at a constant angular velocity of the rotor) and the moments produced by the eccentricity of pressure with respect to CG (M_{xG} , M_{yG} , M_{zG}). The material taken into consideration was an aero engine Ti-alloy, with a Young Modulus of 110 GPa, Poisson's ratio of 0.3 and density equal to 4500 kg/m³. They first carried out an analysis for both the geometries applying just the angular velocity in order to understand the skew effect of the dovetail interface. They then carried out an analysis for each different force acting on the dovetail, another analysis with the application of both centrifugal force and aerodynamic force, and, lastly, an analysis in which all the loads were applied at the same time. They concluded that the skew effect increases the peak contact pressure and slip by a factor of two compared to a straight dovetail slot. This happens because the skew angle generated an additional moment. The skew effect also tends to shift the pressure distribution peak to the lower contact edge, compared to the peak line contact loading obtained from a straight dovetail. The

distributions of other contact variables were also found to be considerably different. On the loaded skewed geometry blade, the contact pressure, slip and surface stresses were found to be significantly higher.

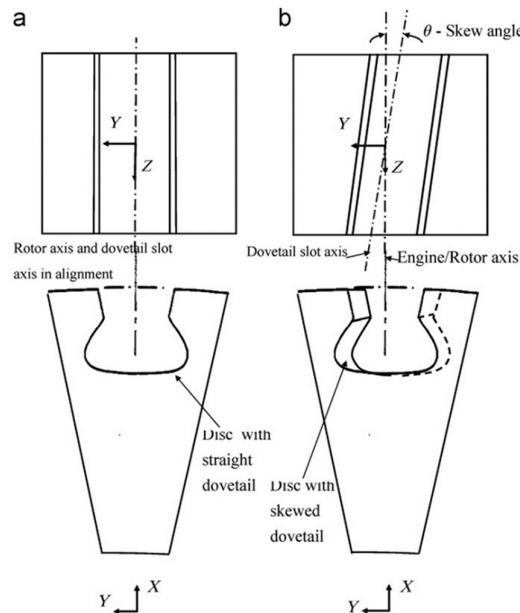


Figure 30. Rotor disk with (a) straight dovetail and (b) skewed dovetail ($\theta = 20^\circ$) [81]. Reprinted with permission from Ref. [81]. Copyright 2022 Elsevier.

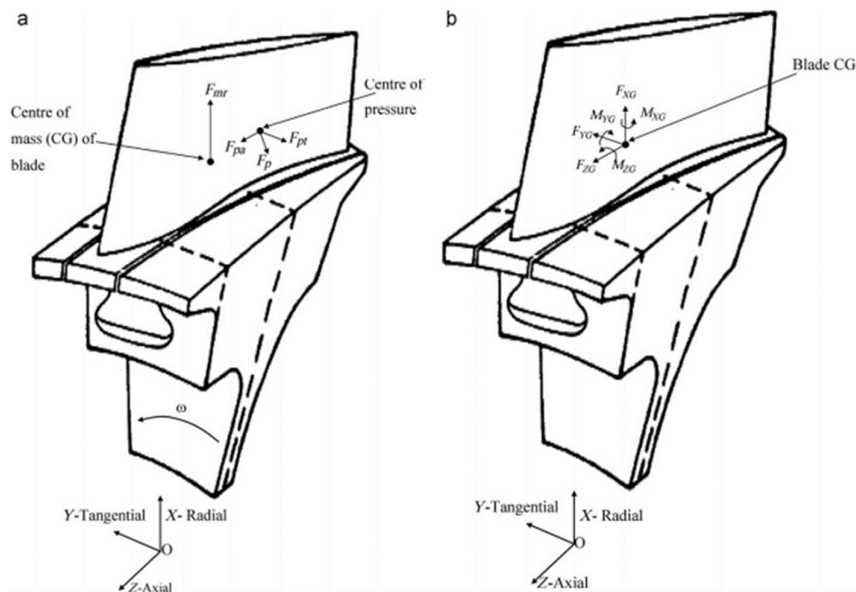


Figure 31. Loads acting on the rotor: (a) centrifugal and aerodynamic loads on the blade and (b) 3D forces and moments at blade CG. Reprinted with permission from Ref. [81]. Copyright 2022, Elsevier.

In a subsequent work [82], they tried to extend and validate the Ruiz criterion in order to evaluate the 3D fretting fatigue damage parameter (*FFDP*). Since three dimensional problems present slip in two directions and six stress components at the interface, they approached the problem in two ways:

- Summation approach: this approach considered the summation of the *FFDP* evaluated for two slip directions;
- Maximum principal-shear stress: this approach considered the use of maximum principal stress in place of σ_T and the replacement of shear stress τ with maximum shear stress considering all the stress components. The formula would then become:

$$FFDP_{3D} = \sigma_1 \cdot \tau_{max} \cdot \delta_{res} \quad (10)$$

where σ_1 is the maximum principal stress, τ_{max} is the maximum shear stress and δ_{res} is the resultant of slip in the two directions.

They evaluated the *FFDP* both ways using the FEM model developed for the previous work, and concluded that the *FFDP* estimation from maximum principal-shear stress approach was more appropriate for three dimensional problems, and that it can be used to identify the fretting fatigue critical location, even though experimental validation of these approaches was strongly suggested.

In 2014, Jayaprakash and Mutoh [83] used the previously developed [84] tangential stress range—compressive stress range (TSR-CSR) generalized diagram (Figure 32) in order to predict the fretting fatigue strength of a dovetail joint. In Figure 32, the normalization equation is reported where NTS is the normalized tangential stress range with respect to the tensile strength, NCS is the normalized compressive stress range with respect to the tensile strength, and 0.28 is the critical stress parameter (CSP) at a fatigue limit of 10^7 cycles.

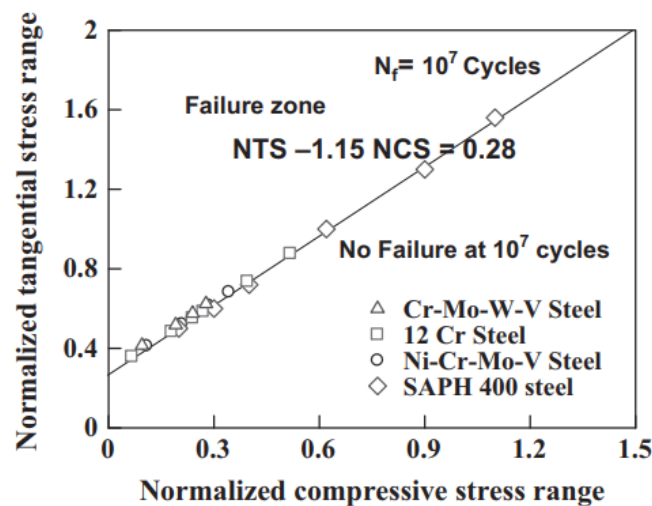


Figure 32. Generalized TSR-CSR diagram for steels [83]. Reprinted with permission from Ref. [83]. Copyright 2022 Elsevier.

For each applied cyclic load, the tangential stress range (TSR) and compressive stress range (CSR) were retrieved by means of a FE model, then they were normalized in order to retrieve NTS and NCS. The generalized TSR-CSR diagram could then be used to predict which cyclic load will be critical for fretting fatigue failure.

To validate the use of this diagram for dovetail joints, they ran experimental tests on a specimen that was geometrically identical to the one used in the FEA. The results are shown in Figure 33, and it can be seen (Figure 33b) that the predicted limit value is in good agreement with the limit value retrieved from the experimental data. It must be highlighted that this general TSR-CSR diagram just used for steels. For other types of materials, the diagram has to be obtained.

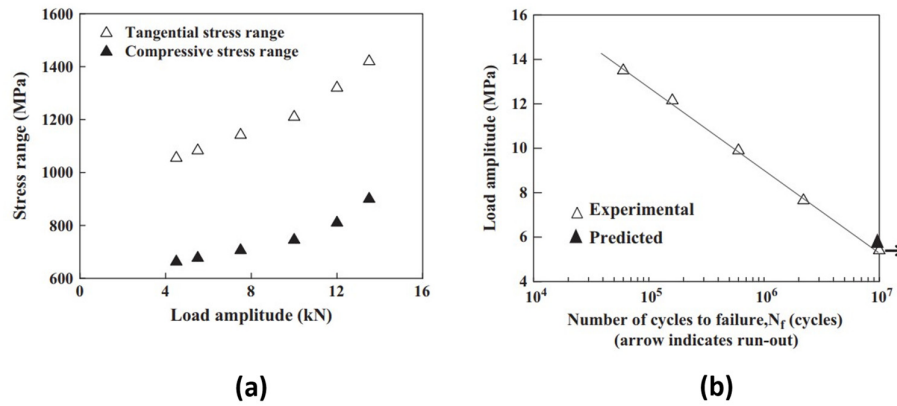


Figure 33. (a) Tangential stress range and compressive stress range with respect to load amplitude (b) S-N curve for the fretting fatigue test of dovetail joint. Reprinted with permission from Ref. [83]. Copyright 2022 Elsevier.

In 2015, Da-Sheng et al. [18] studied the possibility of carrying out a 2D FE analysis on dovetail joints in order to retrieve contact stresses considering the plastic behavior of the material. A viscoplastic constitutive model of the Ti-6Al-4V alloy based on the Chaboche theory [85] was used. The results retrieved in terms of stresses along the contact surface and in the depth direction showed that the cyclic stress characteristics were not the same for different nodes. It was suggested that these differences add complexity to identifying the right parameters to be taken into consideration when designing for fretting fatigue and, therefore, that plasticity behavior should be considered when evaluating contact stresses.

A year later, they conducted an experimental and numerical study on a circular arc Ti-6Al-4V dovetail specimen (Figure 34) in order to investigate its fretting fatigue behavior at three different loading levels [86]. The experimental data in terms of fretting fatigue life were compared with predicted life evaluated by using the multiaxial SWT-critical plane criterion as the contact zone was subjected to a multiaxial stress state ([2,87,88]).

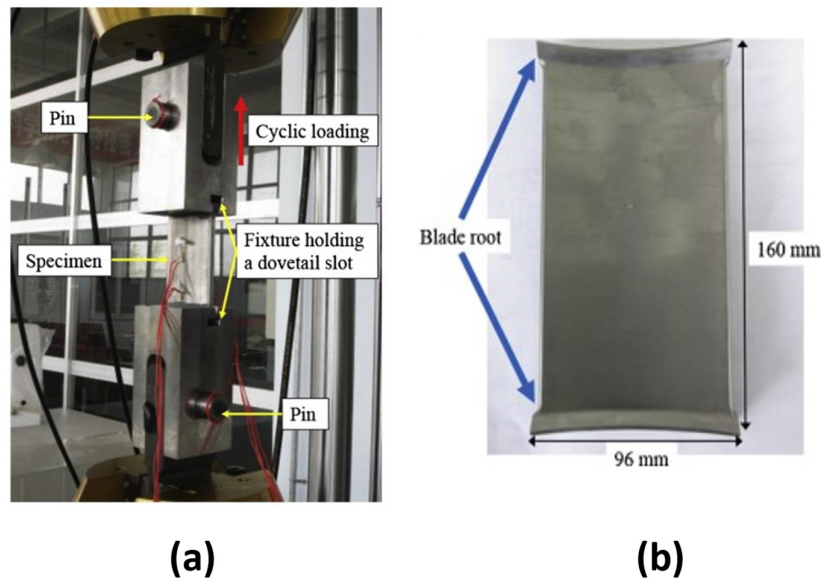


Figure 34. (a) Dovetail test fixture and (b) dovetail specimen used in [86]. Reprinted with permission from Ref. [86]. Copyright 2022 Elsevier.

They compared the results obtained through:

1. traditional SWT parameter ($SWT = \sigma_{max} \cdot \varepsilon_a$ where σ_{max} is the maximum normal stress in one cycle on the critical plane and ε_a is the normal strain amplitude on the critical plane [50]);
2. averaging SWT introducing a weight function since it was reported that crack initiation parameters (such as SWT) provided conservative life predictions in the case of high stress gradients. The averaged SWT parameter is expressed as follows:

$$SWT_{grad} = \frac{1}{W} \times SWT \quad (11)$$

where $W = f(\overline{SWT}) = 1 + \sum_{i=1}^m a_i \cdot (\overline{SWT})^i$ is the weight function used, a_i is a constant which can be fitted by the least squares method with experimental results, $\overline{SWT} = \frac{\Delta SWT}{d} = \frac{SWT_{max}(Y'=0) - SWT(Y'=d)}{d}$ is the mean gradient of SWT , d is defined as the distance between the contact surface and the point where the local gradient reduces to zero (in this case $d = 64 \mu\text{m}$). For further description of the equation see [86].

The results (presented in Figure 35) showed that introducing the weight function greatly enhanced the life prediction accuracy (especially choosing $m = 2$).

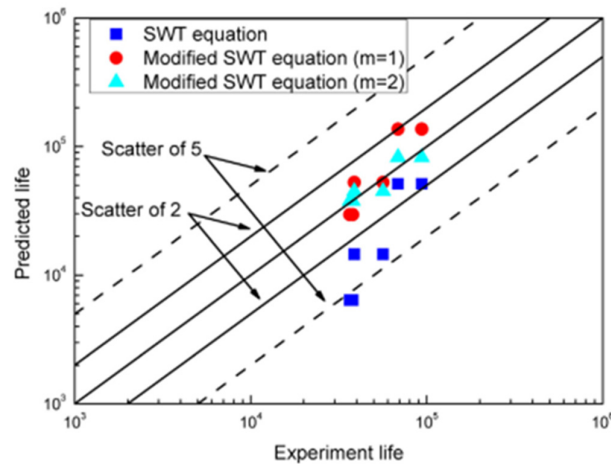


Figure 35. Predicted results using the traditional and the modified SWT equation [86]. Reprinted with permission from Ref. [86]. Copyright 2022 Elsevier.

In 2017, Yang et al. [89] investigated the effect of shot-peening treatment on a Ti-6Al-4V dovetail joint. They tested both shot-peened (SP) specimens and “as-received” (AR) specimens, bringing them to failure, applying an average loading value of 5.5 kN, an amplitude value of 4.5 kN, a stress ratio of 0.1, and a sinusoidal wave of 10Hz frequency. The fixture used is showed in Figure 36.

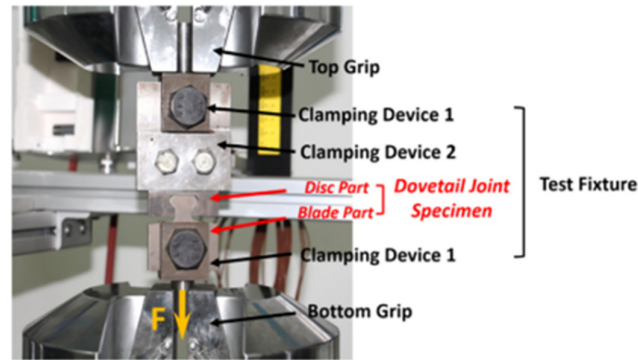


Figure 36. Test fixture used by Yang et al. [89]. Reprinted with permission from Ref. [89]. Copyright 2022 Elsevier.

Observations of the fretting area and fretting cracks were conducted using a scanning electron microscope (SEM). They observed that the shot-peening treatment increased the fretting fatigue life of the specimens by 100% (from an average of 189,574 cycles to an average 379,646 cycles) as shown in Figure 37.

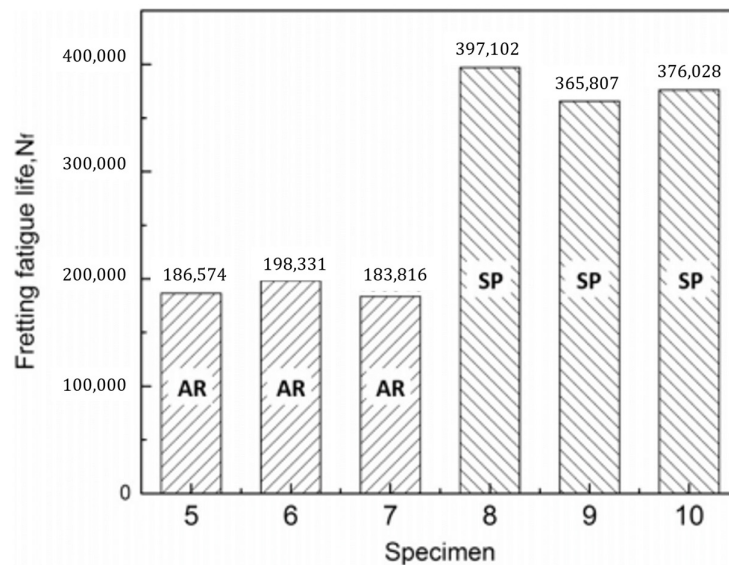


Figure 37. Fretting fatigue life results with AR being the “as-received” specimens and SP being the shot-peened specimens [89]. Reprinted with permission from Ref. [89]. Copyright 2022 Elsevier.

The explanation given was that shot-peening acted both on the resistance to initiation of cracks (by inducing a surface strain-hardening layer that increases the local yield strength) and on the inhibition of crack propagation (by inducing residual compressive stress on the surface layer).

Recently, Mangardich et al. [90] conducted an interesting numerical study on Ti-6Al-4 V dovetail joint models in order to compare results given by the use of either the *SWT* parameter nucleation model or the modified *SWT* parameter nucleation model introduced by Ding et al. [91]. The main difference between the two models is that the second one takes into account the effect of frictional wear:

$$SWT_{mod} = \sigma_{max} \cdot \epsilon_a \cdot D_{fret} \quad (10)$$

with

$$D_{fret} = (1 + \tau\delta)^m \cdot \left(1 - \frac{\tau\delta}{(\tau\delta)_{th}}\right)^n \quad (11)$$

being the damage associated with frictional wear, and $(\tau\delta)_{th}$ being the frictional work threshold above which fretting wear damage is predominant with respect to fretting fatigue damage. They observed that the modified *SWT* model was more precise in terms of the nucleation zone prediction with respect to the plain *SWT* model. It also predicted a fretting fatigue life identical to test results: nonetheless, a single calibration point was used. It was therefore highlighted that this approach has to be further tested for different loading conditions and dovetail attachments in order to be fully validated.

Most Significant Results

The most important results from the studies in this section may be summarized as:

- Different dovetail skew angles were not found to substantially influence fretting fatigue life;
- Coatings and shot-peening were found to be effective for raising the resistance to fretting fatigue crack initiation. More types of coatings should be tested in order to give better guidelines;
- Analytical studies indicate that smaller punch radiuses are expected to improve fretting fatigue behaviour, but it was highlighted that the effect of vanishing small radiuses is unknown and therefore that research on the matter is needed;
- The Ruiz criterion successfully located the initiation location, but it was highlighted that the parameters used by Ruiz do not have a direct physical interpretation and, therefore, are not generally suitable for quantitative analyses. Other parameters have been mathematically developed, although validation on different geometries is currently lacking;
- The use of the *SWT* criterion, especially in its weighted variant [86] and modified variant [91] were found to be able to successfully predict crack nucleation site on specimens. The modified variants also successfully predicted the fretting fatigue life of specimens. However, it was highlighted that these approaches must be further tested under different loading conditions in order to be fully validated;
- The TSR-CSR diagram was found to be a useful tool for the prediction of fretting fatigue failure, even though it is different for every material, and so it has to be retrieved for each material tested or used;
- The linear elastic fracture mechanics (LEFM) approach was also found to be generally a good tool for the evaluation and prediction of crack growth lives;

4. Bolted Joints

As it is widely known, a huge amount of structural parts are fastened with bolts and rivets, as they are able to resist high levels of structural loads, allowing different materials to be joined and (for bolts) allowing for joint disassembly. These mechanical components are particularly subjected to a high stress raise due to the presence of geometrical discontinuities at holes and therefore to fatigue crack initiation. Moreover, bolted joints might suffer from fretting fatigue damages occurring at the contacting surfaces of the joint, due to the very small relative displacements occurring between the bodies.

The first study on fretting fatigue damage in bolted joints was conducted by Sandifer in 1973 [92]. He carried out a series of tests on an aluminum 2024-T3 double lap joint specimen (Figure 38) aiming at developing design methods in order to reduce fretting on the joint. The connection has been tested by inserting different materials at the interface, and it was concluded that shot-peening and bonding the surface would bring an improvement both in fatigue life and fretting reduction. However, application constraints require the parts to be easily dismountable, and therefore bonding would be a limitation.

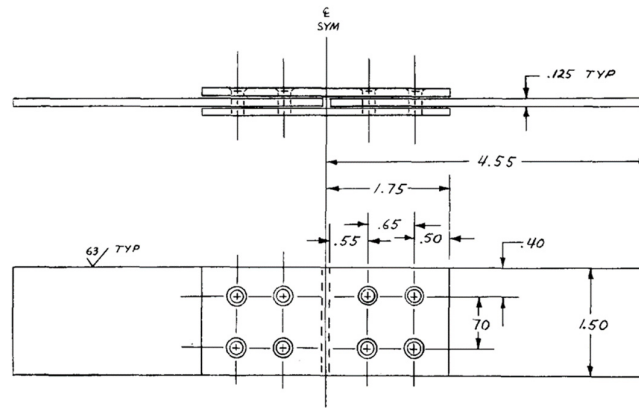


Figure 38. Double lap joint specimen [92]. Reprinted with permission from Ref. [92]. Copyright 2022 Elsevier.

In 2009, Wagle and Kato [93] ran a series of experiments again on aluminium alloy plates 2024-T3 in order to investigate the effect of tightening torque on fretting. Two different specimens were tested (Figure 39): the bolt hole specimen was tested by applying load at one of the bolt hole edges by means of a steel pin, while, on the bolted specimen, the load was applied by clamping the edges of the specimen to a press.

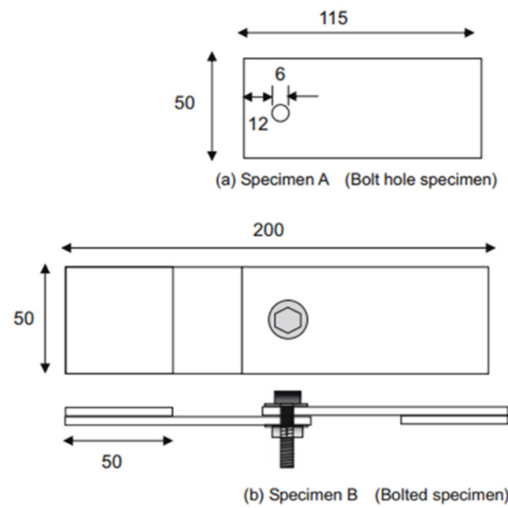


Figure 39. (a) Bolt hole and (b) bolted specimen [93]. Reprinted with permission from Ref. [93]. Copyright 2022 Elsevier.

They observed three different mechanisms of failure depending on the tightening torque and the stress amplitude as shown in Figure 40. For low tightening torque values, traditional mechanical fatigue damage occurred (MF), for medium range tightening torque values, fretting wear damage occurred (FW), and for high tightening torque values, fretting fatigue (FF) occurred. In general, the fatigue life increased with an increasing tightening torque for the MF and FW ranges, while the contrary is true for the FF range.

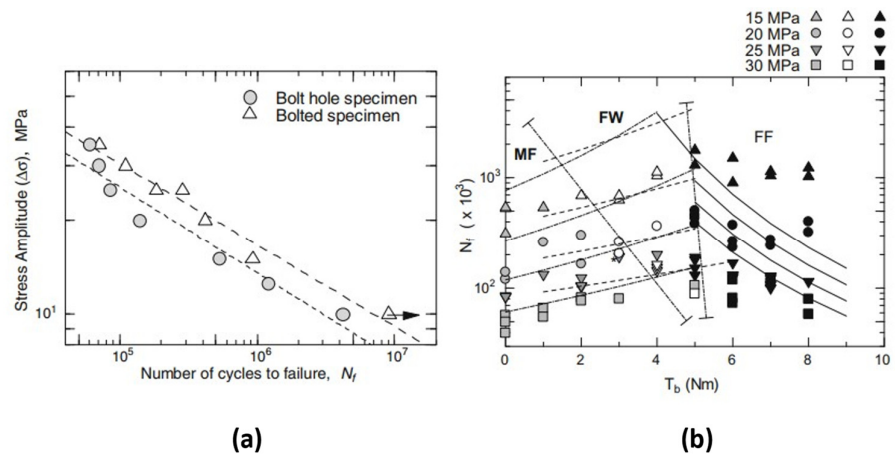


Figure 40. (a) S-N curve retrieved by the experimental data and (b) change in fatigue life depending on tightening torque T_b at different stress amplitude [93]. Reprinted with permission from Ref. [93]. Copyright 2022 Elsevier.

During the same year, Zografos et al. [94] developed a 2D analytical model of the bolted connection in a wheel set up for a “cornering test” (Figure 41), to characterize the macroscopic behaviour of the joint and to predict the contact stresses at the interface. They divided the overall investigation into three levels:

1. Evaluation of the general response of the bolted joint when rotating bending and other remote loading conditions are applied (macroscopic response—level 1);
2. Evaluation of the contact traction at the interface between the parts in contact (contact interactions and interface characterisation—level 2);
3. Evaluation of the full stress field near the critical damage areas (stress field or local response—level 3).

The full method flowchart is shown in Figure 42.

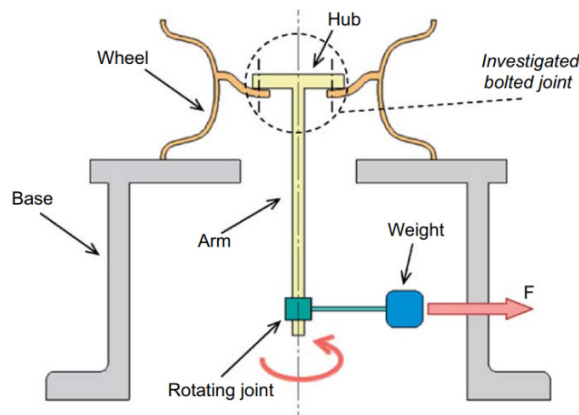


Figure 41. Cornering test apparatus [94]. Reprinted with permission from Ref. [94]. Copyright 2022 Elsevier.

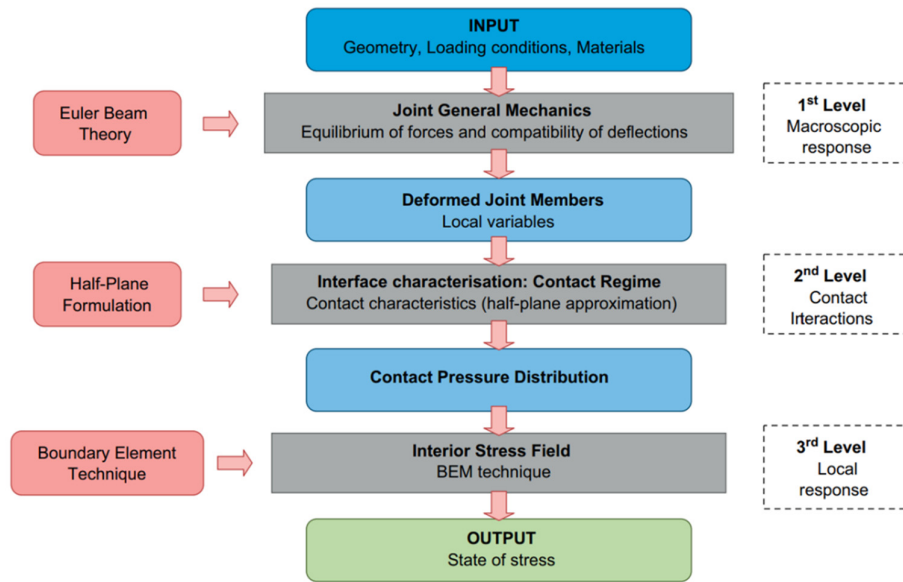


Figure 42. Model flow chart [94]. Reprinted with permission from Ref. [94]. Copyright 2022 Elsevier.

The model correctly predicted the macroscopic behaviour and the local contact interactions, even though this model alone does not give enough information to be able to produce a direct assessment of an assembly. The study highlighted the importance of many parameters, such as the distance of the bolts from the hub outer diameter, the bolt preload and the equivalent bolt spring stiffness. It is suggested that a multi-variable parametric study is necessary in order to correctly design this type of connection. This work did not contemplate frictional contact, which might be implemented in the model.

A couple of years later, Jayaprakash et al. [95] investigated the possibility of predicting the fretting fatigue life of an S355mc (hot rolled low-alloy steel) automotive bolted joint using the tangential stress range (TSR)-compressive stress range (CSR) diagram previously developed by them [84,96].

They first carried out a series of fatigue tests on the joint and they investigated the effect of the presence of a groove at the contact edge (Figure 43).

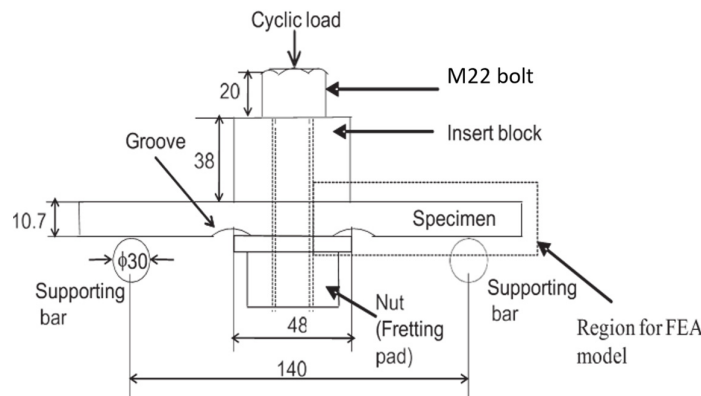


Figure 43. Schematic drawing of the bolted plate specimen [95]. Reprinted with permission from Ref. [95]. Copyright 2022 Elsevier.

They then retrieved the TSR-CSR diagram by testing conventional laboratory-type S355mc specimens on a bridge-type fretting fatigue test rig. The maximum value of the tangential stress range and the value of the compressive stress range corresponding to the

point of maximum tangential stress range were retrieved by using a FEA model (Figure 44).

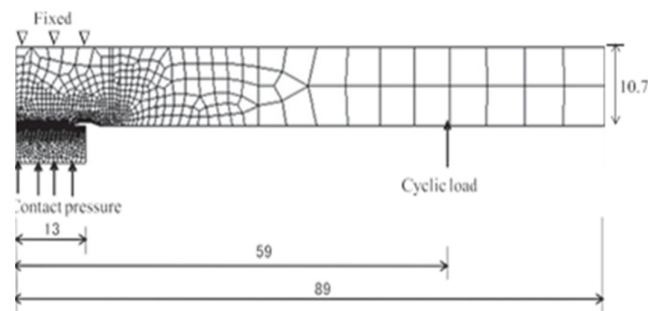


Figure 44. FEM analysis submodel [95]. Reprinted with permission from Ref. [95]. Copyright 2022 Elsevier.

They observed that introducing a groove at the contact edge improved the fretting fatigue life of the joint, the deeper the groove the higher the fretting fatigue strength retrieved. They found a linear relationship between TSR and CSR at each fretting fatigue life in the laboratory type specimen, which gave a fretting fatigue failure criterion: failure will not occur when the combination of TSR and CSR is below the line.

The data point retrieved from the bolted specimens agreed with the TSR-CSR diagram retrieved by testing the laboratory type specimens (Figure 45). Therefore, it is implied that the TSR-CSR diagram can be used as a fretting fatigue design curve.

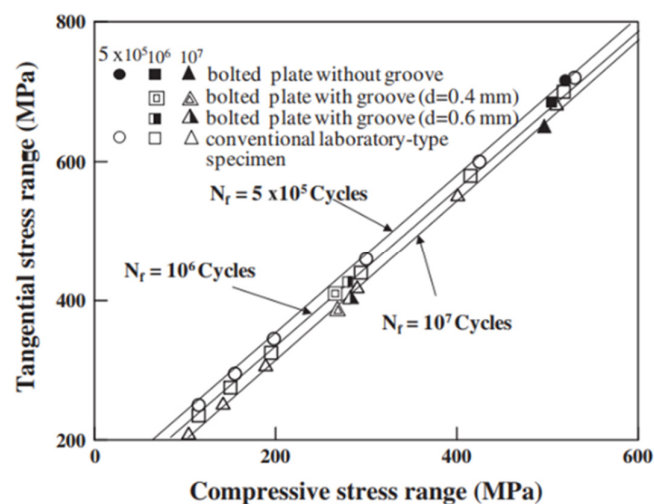


Figure 45. TSR-CSR diagram for S355mc [95]. Reprinted with permission from Ref. [95]. Copyright 2022 Elsevier.

Chakherlou et al. [19,97] carried out an experimental and numerical investigation in order to study the bolt clamping force and friction coefficient influence on the fretting fatigue behaviour of a 2024-T3 aluminium alloy double shear lap joint. They first run a series of fretting fatigue tests at three different values of tightening torques (0.25 Nm, 2 Nm and 4 Nm) on the specimen showed in Figure 46a. Tests were run with and without lubricant applied between the plates. Tests with the application of clearance fit pins instead of bolts were also run, in order to compare the results with the specimens tightened with the lowest tightening torque.

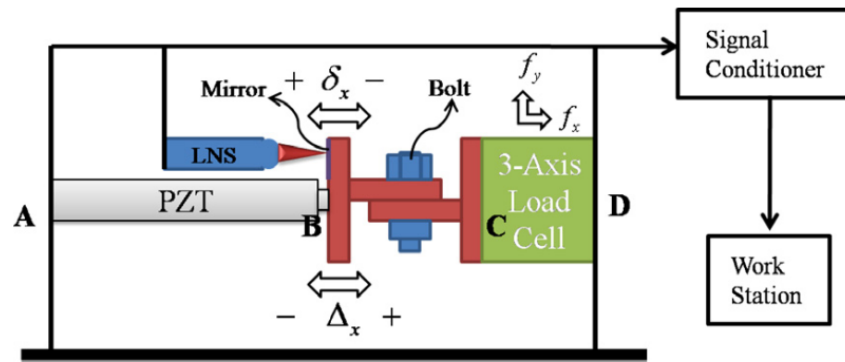


Figure 48. Schematic drawing of the developed bolted joint fixture [99]. Reprinted with permission from Ref. [99]. Copyright 2022 Springer Nature.

The laser nanosensor (LNS in the picture) measures the relative motion between the mating surfaces. One very important aspect of this fixture design is that no post-processing and filtering is needed to obtain the fretting response.

In 2012, Benhamena et al. [100] first used a material response fretting map (MRFM) in order to describe the fretting behaviour of a bolted joint specimen. In the first part of the work, an experimental investigation on 5086H24 (work hardened by rolling, and then annealed to half hard) aluminium alloy plates was presented. The testing apparatus is shown in Figure 49. They tested the joint with six selected levels of contact force (0 kN, 4 kN, 6 kN, 8 kN, 10 kN and 12 kN).

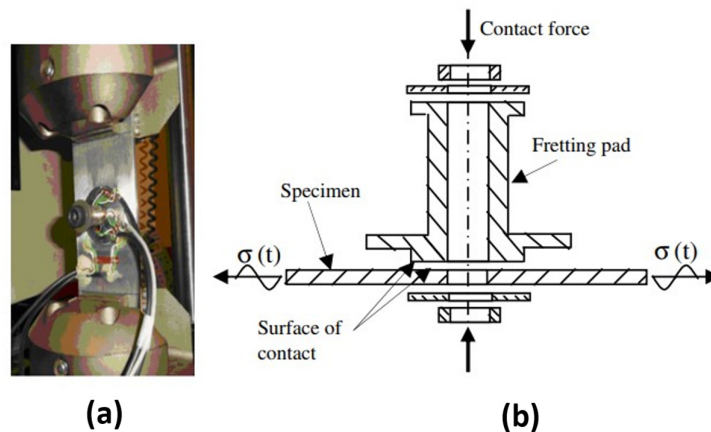


Figure 49. (a) Test fixture and (b) schematic drawing of the bolted joint specimen used [100]. Reprinted with permission from Ref. [100]. Copyright 2022 Elsevier.

Besides the recurring observation that a higher tightening torque improved the fretting fatigue behaviour of the joint, the SEM observations highlighted that with increasing contact forces, the site of crack initiation would vary from the edge of the hole to the border of the contact.

In order to visually describe and analyse the different experimental conditions, they built a MRFM (shown in Figure 50) that highlighted how the mechanism of fretting fatigue not only depended on local stress but also strongly depended on relative displacement. The three areas shown in the map described the different behaviours of the specimens for different combinations of contact stresses and relative displacements: the cracking area of

the graph indicates the fretting fatigue damage area, while the wearing area indicated the fretting wear damage area.

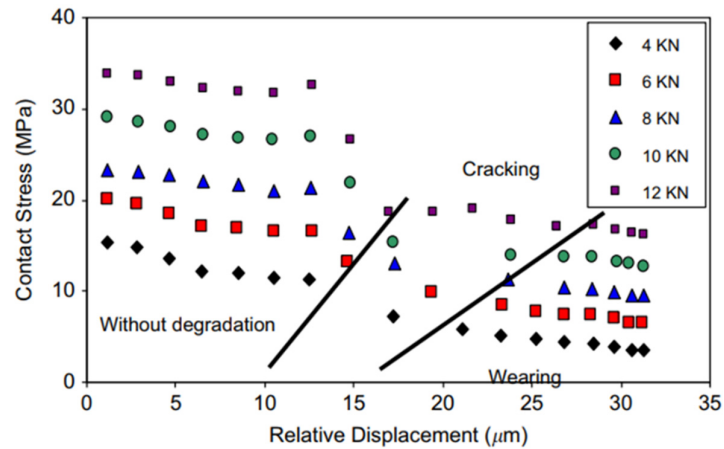


Figure 50. Material response fretting map (MRFM) for 5086H24 aluminium alloy [100]. Reprinted with permission from Ref. [100]. Copyright 2022 Elsevier.

In the same year, Oskouei and Ibrahim [101] conducted a study on the fretting fatigue behaviour of Ni-P coated Al 7075-T6 bolted plates. They tested double-lap bolted joint specimens (shown in Figure 51) at different tightening torques (5 Nm and 8 Nm) both uncoated and coated (thickness of approximately 40 μm).

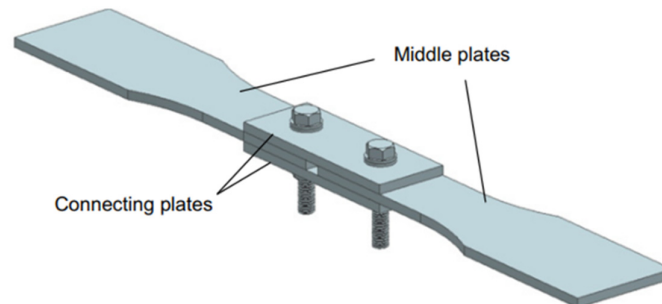
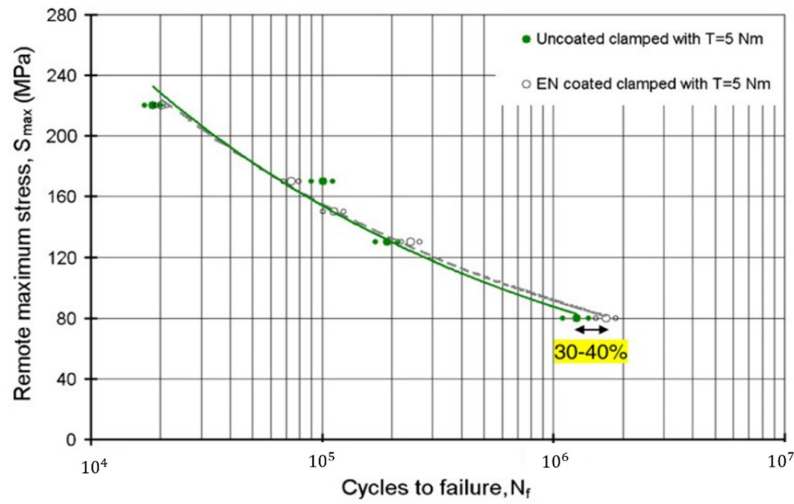


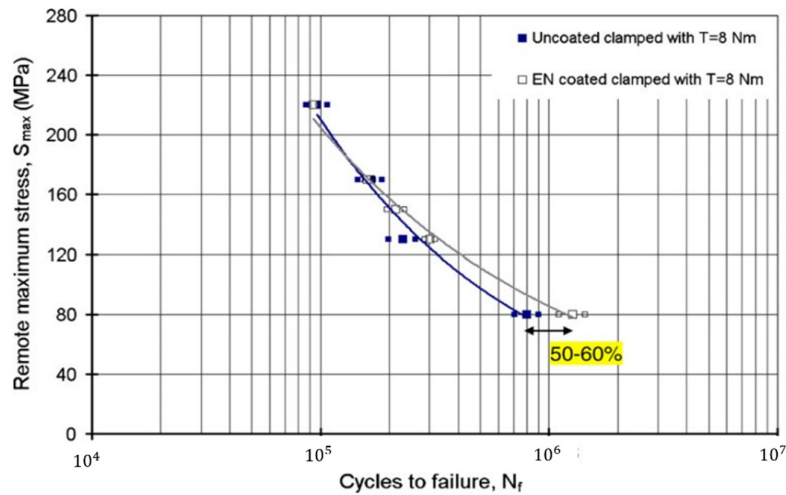
Figure 51. Double lap bolted joint specimen used [101]. Reprinted with permission from Ref. [101]. Copyright 2022 Elsevier.

The behaviour of the joints was found to be strongly dependent on both applied tightening torque and maximum alternating load. They reported that the application of Ni-P coatings successfully protected the specimen against fretting fatigue, improving their life by 30–40% in the case of a tightening torque equal to 5 Nm and by 50–60% in

the case of a tightening torque of 8 Nm (Figure 52).



(a)



(b)

Figure 52. S-N curves for uncoated and coated Al 7075-T6 bolted joint specimens clamped with (a) $T = 5$ Nm and (b) $T = 8$ Nm, at $R = 0.1$ [101]. Reprinted with permission from Ref. [101]. Copyright 2022 Elsevier.

In 2015, Ferjaoui et al. [102] developed a numerical-analytical model that could help analyze the crack initiation phase and predict the crack initiation lifetime of double bolted lap joints. They run experimental tests on double lap bolted specimens (Figure 53), following the ASTM E2789-10 standard [103], using identical Al 2024-T3 plates at different external axial loading conditions (14 kN, 16 kN, 18 kN and 20 kN).

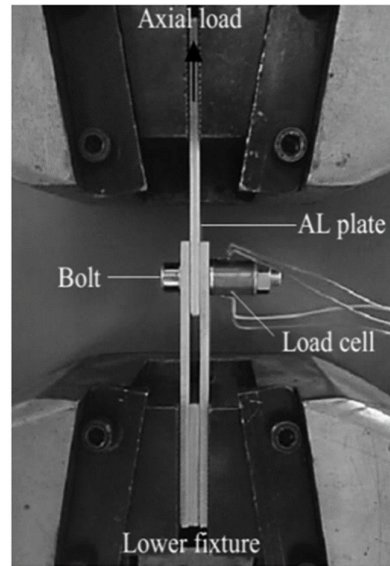


Figure 53. Double lap bolted joint fixture used [102]. Reprinted with permission from Ref. [102]. Copyright 2022 Elsevier.

They then run an FE analysis (the model is shown in Figure 54) on ABAQUS in order to develop a tool to estimate fretting fatigue crack initiation lifetime. The analyses also provided information in terms of local relative slip and stress distributions that would not be possible to retrieve from the experimental tests. Again, the importance of slip amplitude with respect to fretting fatigue life was underlined.

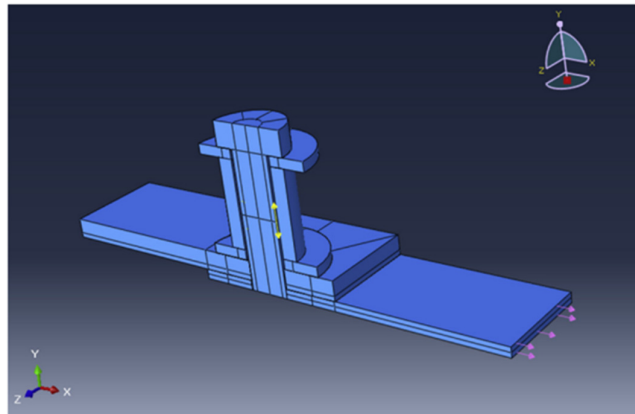


Figure 54. Double lap bolted joint model used [102]. Reprinted with permission from Ref. [102]. Copyright 2022 Elsevier.

They then applied a continuum damage mechanics (CDM) approach in conjunction with FEA in order to determine the crack initiation lifetime of the double bolted lap joint. An uncoupled damage evolution law was derived for high cycle fatigue, and further explanation of the analytical model used can be found in the paper [102].

Figure 55 shows the comparison between the data retrieved from the experimental campaign and the predicted results. A good agreement between the two results can be noted.

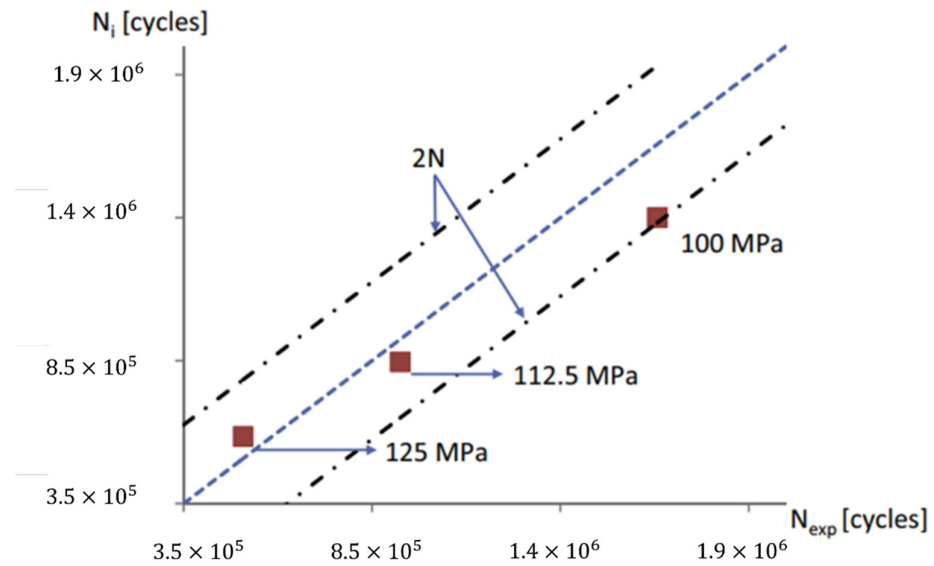


Figure 55. Predicted results versus experimental results for fretting fatigue crack initiation [102]. Reprinted with permission from Ref. [102]. Copyright 2022 Elsevier. More recently, an investigation of fretting fatigue behaviour in high strength steel S500MC was conducted by Jiménez-Peña et al. [104]. A series of experimental tests was carried out on single lap bolted joint specimens, using different pre-tension levels (200 Nm, 300 Nm and 350 Nm) and applying different axial loads (30 kN, 35 kN, 40 kN and 50 kN). The test apparatus is shown in Figure 56.

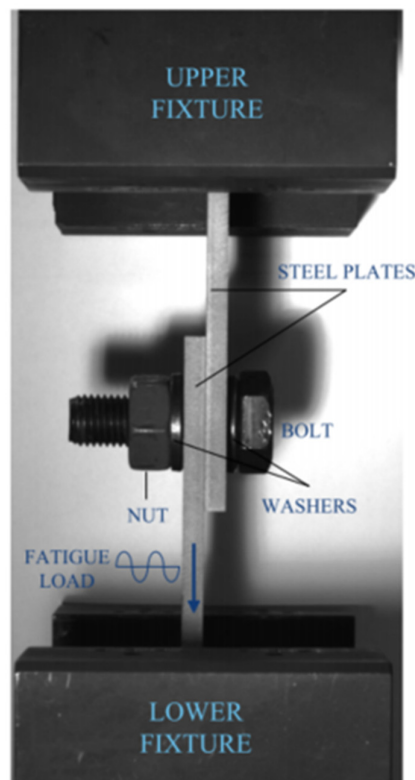


Figure 56. Test apparatus used [104]. Reprinted with permission from Ref. [104]. Copyright 2022 Elsevier.

Again, it was observed that an increase in pre-tension force significantly improved the fatigue life of the connection. A representative 3D-FEA model (Figure 57a) was built in order to study four different fretting fatigue criteria: the *SWT* criterion [50], the Fatemi-Socie (*FS*) criterion ($FS = \frac{\Delta\gamma}{2} \left(1 + \alpha \cdot \frac{\sigma_{max}}{\sigma_y}\right)$ where $\Delta\gamma$ is the maximum shear strain range, σ_{max} is the maximum normal stress in one cycle, σ_y is the yield stress and α can be approximated to 0.5 [51]), the Crossland [105] criterion and the Ruiz criterion [59]. All the criteria showed similar results in terms of crack nucleation location (as shown in Figure 58), though only the Ruiz criterion was able to follow the beneficial effect of the tightening torque (*FFDP* diminished as the tightening torque increased). This is probably because the other three parameters need to be correlated with the relative slip amplitude occurring, since it has been proven to be determinant in influencing the fretting behaviour of joints [106].

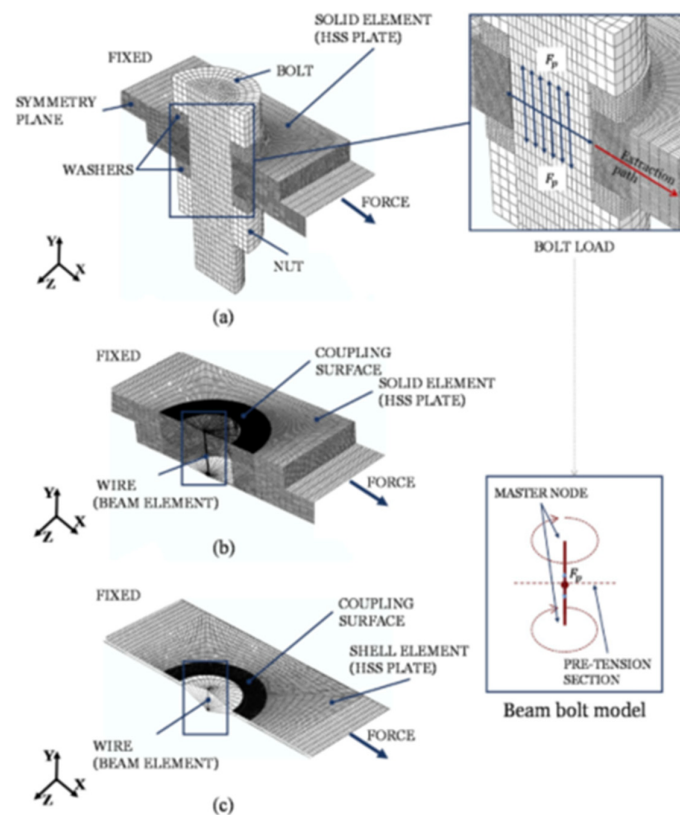


Figure 57. Finite element models for the single lap bolted joint: (a) full solid model, (b) solid equivalent model and (c) shell equivalent model [107]. Reprinted with permission from Ref. [107]. Copyright 2022 Elsevier.

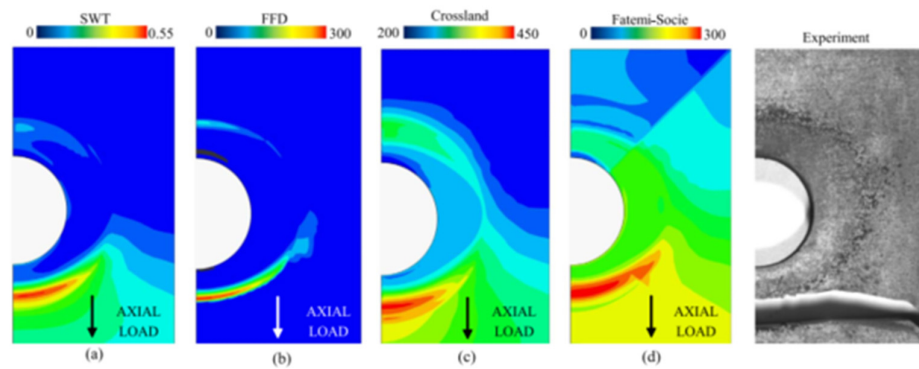


Figure 58. Multi-axial parameter results for (a) SWT, (b) Ruiz's *FFDP*, (c) Crossland and (d) *FS* [104]. Reprinted with permission from Ref. [104]. Copyright 2022 Elsevier.

In a subsequent work [107], they developed and validated two simplified FE models aiming at saving computational time. The two models are showed in Figure 57a,b. Both simplified models turned out to accurately predict the material fretting response, and were therefore validated (Figure 59a). It was evaluated that using the shell equivalent model saved up to 97.1% of computational time (Figure 59b).

Over the last few years, Mäntylä et al. [108–113] kept on researching the subject of fretting fatigue. In particular, they developed a contact model that takes into consideration the evolution of the local coefficient of friction and of wear under fretting conditions in bolted joints. The contact model can be integrated in FEM software by introducing a subroutine. The subroutine includes both the local friction evolution (by evaluating the frictional energy dissipation) and wear (by implementing Archard's equation) modeling. It was pointed out, however, that despite giving an estimation of the contact loosening and eventual failure, the model is very conservative due to the fact that Archard's wear model does not consider the wear particle entrapment inside the contact.

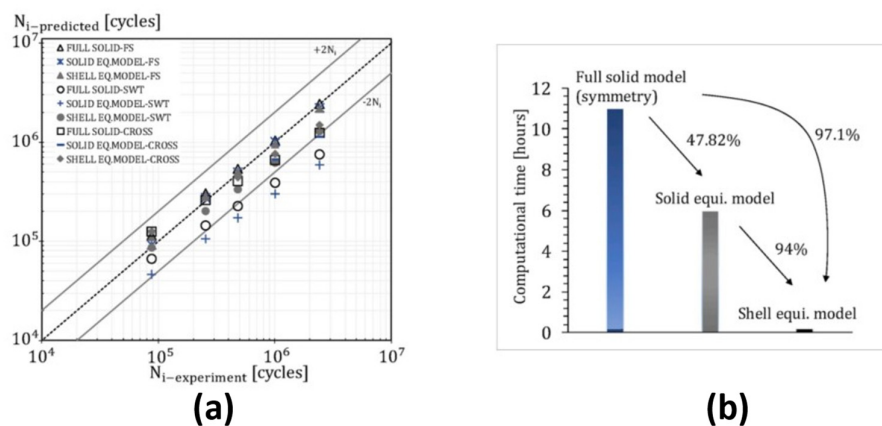


Figure 59. (a) Predicted fretting fatigue life results of the various numerical models compared to the experimental results and (b) saved computational time [107]. Reprinted with permission from Ref. [109]. Copyright 2022 Elsevier.

Most Significant Results

The analysis of bolted joints studies draws some important conclusions:

- In fretting contact conditions, increasing the tightening torque is generally a good approach for improving fretting fatigue life. This is explicable with the consequent lowering of sliding happening in the contact area;

- It has also been highlighted that, for low tightening torques, fretting fatigue does not occur. This can be visually explained by means of fretting maps, like the one used by Benhamena et al. [100]. It has been found that for low contact loads, and regardless of high or even very low slipping, fretting fatigue might not occur. For more information about fretting maps, please refer to [108,114–116];
- Bonding the mating surfaces does improve fatigue life, but is a limitation affecting the disassembly of the joint;
- Use of fretting fatigue criteria such as the *SWT*, the *FS* and the Ruiz criterion was found to be useful to identify the crack nucleation location. More research is needed in order to assess the use of these parameters;
- Applying Ni-P coatings was proven to improve fretting fatigue life;
- Applying lubrication between the contact surfaces has been reported to have mixed results. The results may arise from different initial experimental conditions. More studies need to be carried out, in order to assess more clearly the advantages and disadvantages of the use of lubricants;
- The TSR-CSR diagram was found to be a useful tool for the prediction of fretting fatigue failure also for bolted joints.

5. Conclusions

This review aimed at giving a comprehensive insight into fretting fatigue practical problems and solutions up until the present. However, it is by no means complete: it is very clear how solutions and evidence are sometimes not univocal, and are sometimes even in contrast with each other. In general, it can be concluded that:

- Under fretting conditions, cracks develop near the edge of the contact area, corresponding to the peak contact stress. However, if fretting wear occurs, cracks have been reported to initiate at the inner surface of contact area because of peak stresses occurring at the edge of the wear scar. At the same time, fretting crack initiation at the contact edge is significantly reduced because of the cracks getting ground off;
- Relative slip and contact pressure are fundamental parameters that directly influence, together with wear, the local stress–strain contact state. Therefore, evaluating the joint action of these parameters is important for predicting the macroscopic behavior of the joint, as different combinations can lead either to an improvement or a deterioration of fretting fatigue life;
- Multiaxial fatigue parameters used with the critical plane approach (as *SWT* and *FS*) appear to be helpful in locating fretting fatigue crack initiation location for all kind of joints. However, the total predicted life is strongly influenced by the choice of the initial crack length, which is arbitrary;
- The TSR-CSR diagram was found to be a useful tool for the prediction of fretting fatigue failure both in dovetail and bolted joints. Research for the application of this criterion on press-fitted shaft/hub joints is lacking, however, and is therefore needed. It must also be highlighted that the TSR-CSR diagram is different for each material and so it must be retrieved for any new, used or tested material;
- The application of the linear elastic fracture mechanics (LEFM) approach was also found to be optimal for the evaluation and prediction of crack growth lives for all the joints covered in this review;
- Coatings and shot-peening were found to be effective for raising the resistance to fretting fatigue crack initiation. More types of coatings should be tested, however, since the results refer to a very limited group of treatments; fretting maps are also very useful and easy to read tools that can give a visual and immediate description of the fretting regime (or lack of) occurring in the joint.

The research paths and main results have been presented but, as previously highlighted, further research for the validation of all the identified criteria is still needed,

since no complete and universal description of the effects of fretting and design method has been produced.

Author Contributions: Writing—original draft preparation, C.S.; writing—review and editing, M.D.A.; supervision, D.C., S.F., G.O. and F.R. All authors have read and agreed to the published version of the manuscript.

Funding: This research received no external funding.

Institutional Review Board Statement: Not applicable.

Informed Consent Statement: Not applicable.

Data Availability Statement: Not applicable.

Conflicts of Interest: The authors declare no conflict of interest.

References

- Hurricks, P.L. The Mechanism of Fretting—A Review. *Wear* **1970**, *15*, 389–409. [https://doi.org/10.1016/0043-1648\(70\)90235-8](https://doi.org/10.1016/0043-1648(70)90235-8).
- Szolwinski, M.P.; Farris, T.N. Mechanics of Fretting Fatigue Crack Formation. *Wear* **1996**, *198*, 93–107.
- Nishioka, K.; Hirakawa, K. Fundamental Investigations of Fretting Fatigue: Part 3, Some Phenomena and Mechanisms of Surface Crack. *Bull. JSME* **1969**, *12*, 397–407.
- Nowell, D.; Hills, D.A. Crack Initiation Criteria in Fretting Fatigue. *Wear* **1990**, *136*, 329–343.
- Sunde, S.L.; Berto, F.; Haugen, B. Predicting Fretting Fatigue in Engineering Design. *Int. J. Fatigue* **2018**, *117*, 314–326. <https://doi.org/10.1016/j.ijfatigue.2018.08.028>.
- Hills, D.A.; Dini, D. A Review of the Use of the Asymptotic Framework for Quantification of Fretting Fatigue. *J. Strain Anal. Eng. Des.* **2016**, *51*, 240–246. <https://doi.org/10.1177/0309324716638968>.
- Barber, J.R.; Davies, M.; Hills, D.A. Frictional Elastic Contact with Periodic Loading. *Int. J. Solids Struct.* **2011**, *48*, 2041–2047. <https://doi.org/10.1016/j.ijsolstr.2011.03.008>.
- Hertz, H. Über Die Berührung Fester Elastischer Körper. *J. Für Die Reine Und Angew. Math.* **1881**, *171*, 156–171.
- Johnson, K.L. *Contact Mechanics*; Cambridge University Press: Cambridge, UK, 1989; Volume 37, pp. 29–43. <https://doi.org/10.1201/b17588-12>.
- Cattaneo, C. Sul Contatto Di Due Corpi Elastici: Distribuzione Locale Degli Sforzi. *Accad. Naz. Dei Lincei* **1996**, *6*, 342–349.
- Cattaneo, C. Teoria Del Contatto Elastico in Seconda Approssimazione. *Rend. Di Mat. E Delle Sue Appl. Ser. V* **1947**, *6*, 504–512.
- Cattaneo, C. Teoria Del Contatto Elastico in Seconda Approssimazione: Compressione Obliqua. In *Rendiconti Seminario Facoltà di Scienze Università di Cagliari*; Editoriale Italiana: Roma, Italia, 1947; pp. 13–28.
- Mindlin, R.D. Compliance of elastic bodies in contact. *J. Appl. Mech.* **1949**, *16*, 259–268.
- Mindlin, R.D.; Mason, W.P.; Osmer, T.F.; Dereciwicz, H. Effects of an Oscillatory Tangential Force on the Contact Surfaces of Elastic Spheres. In Proceedings of the 1st National Congress of Applied Mechanics, Chicago, IL, USA, 11–16 June 1951; ASME: New York, NY, USA, 1952; pp. 203–208.
- Mindlin, R.D.; Dereciwicz, H. Elastic Spheres in Contact under Varying Oblique Forces. *J. Appl. Mech.* **1953**, *75*, 327–344.
- Ciavarella, M. The Generalized Cattaneo Partial Slip Plane Contact Problem. II—Examples. *Int. J. Solids Struct.* **1998**, *35*, 2363–2378. [https://doi.org/10.1016/S0020-7683\(97\)00155-8](https://doi.org/10.1016/S0020-7683(97)00155-8).
- Hills, D.A.; Nowell, D. *Mechanics of Fretting Fatigue Tests*; Springer: Dordrecht, The Netherlands, 1994; Volume 29, pp. 153–167. https://doi.org/10.1007/978-94-015-8281-0_7.
- Wei, D.S.; Shi, L.; Wang, Y.R. Cyclic Plastic Behavior of Dovetail under Fretting Load. *Eng. Fail. Anal.* **2015**, *55*, 100–114. <https://doi.org/10.1016/j.engfailanal.2015.05.009>.
- Chakherlou, T.N.; Razavi, M.J.; Abazadeh, B. Finite Element Investigations of Bolt Clamping Force and Friction Coefficient Effect on the Fatigue Behavior of Aluminum Alloy 2024-T3 in Double Shear Lap Joint. *Eng. Fail. Anal.* **2013**, *29*, 62–74. <https://doi.org/10.1016/j.engfailanal.2012.11.004>.
- Farrahi, G.H.; Tirehdast, M.; Masoumi Khalil Abad, E.; Parsa, S.; Motakefpoor, M. Failure Analysis of a Gas Turbine Compressor. *Eng. Fail. Anal.* **2011**, *18*, 474–484. <https://doi.org/10.1016/j.engfailanal.2010.09.042>.
- Kermanpur, A.; Sepehri Amin, H.; Ziaei-Rad, S.; Nourbakhshnia, N.; Mosaddeghfar, M. Failure Analysis of Ti6Al4V Gas Turbine Compressor Blades. *Eng. Fail. Anal.* **2008**, *15*, 1052–1064. <https://doi.org/10.1016/j.engfailanal.2007.11.018>.
- Fonte, M.; Freitas, M.; Reis, L. Failure Analysis of a Damaged Diesel Motor Crankshaft. *Eng. Fail. Anal.* **2019**, *102*, 1–6. <https://doi.org/10.1016/j.engfailanal.2019.04.025>.
- Gutkin, R.; Alfredsson, B. Growth of Fretting Fatigue Cracks in a Shrink-Fitted Joint Subjected to Rotating Bending. *Eng. Fail. Anal.* **2008**, *15*, 582–596. <https://doi.org/10.1016/j.engfailanal.2007.04.003>.
- Wei, D.S.; Di Ma, M.; Zhang, H.; Hu, C.; Wang, Y.R. Study of the Variation of Contact State near the Contact Boundary in a Dovetail Attachment under Different Loads. *Eng. Fail. Anal.* **2019**, *105*, 518–526. <https://doi.org/10.1016/j.engfailanal.2019.07.025>.
- Gürer, G.; Gür, C.H. Failure Analysis of Fretting Fatigue Initiation and Growth on Railway Axle Press-Fits. *Eng. Fail. Anal.* **2018**, *84*, 151–166. <https://doi.org/10.1016/j.engfailanal.2017.06.054>.

26. Wei, D.S.; Yuan, S.H.; Wang, Y.R. Failure Analysis of Dovetail Assemblies under Fretting Load. *Eng. Fail. Anal.* **2012**, *26*, 381–396. <https://doi.org/10.1016/j.engfailanal.2012.06.007>.
27. Scapocchi, C. Fretting Fatigue Analysis in Aluminium Components for Motorcycle Applications, Masters Degree Thesis, University of Bologna, Bologna, Italy, 2019.
28. Kubota, M.; Niho, S.; Sakae, C.; Kondo, Y. Effect of Understress on Fretting Fatigue Crack Initiation. *JSME Int. J.* **2003**, *46*, 220–225.
29. Lee, D.H.; Kwon, S.J.; Ham, Y.S.; You, W.H. Characterization of Fretting Damage in a Press-Fitted Shaft below the Fretting Fatigue Limit. *Procedia Eng.* **2010**, *2*, 1945–1949. <https://doi.org/10.1016/j.proeng.2010.03.209>.
30. Nishioka, K.; Nishimura, A.; Hirakawa, K. Fundamental Investigations of Fretting Fatigue: Part 1, On the Relative Slip Amplitude of Press-Fitted Axle Assemblies. *Bull. JSME* **1968**, *11*, 437–445.
31. Nishioka, K.; Hirakawa, K. Fundamental Investigations of Fretting Fatigue: Part 2, Fretting Fatigue Testing Machine and Some Test Results. *Bull. JSME* **1969**, *12*, 364–370.
32. Nishioka, K.; Hirakawa, K. Fundamental Investigations of Fretting Fatigue: Part 4, The Effect of Mean Stress. *Bull. JSME* **1969**, *12*, 408–414.
33. Nishioka, K.; Hirakawa, K. Fundamental Investigations of Fretting Fatigue: Part 6, Effects of Contact Pressure and Hardness of Materials. *Bull. JSME* **1972**, *15*, 135–144.
34. Nishioka, K.; Komatsu, H. Researches on Increasing the Fatigue Strength of Press-Fitted Shaft Assembly. *Bull. JSME* **1967**, *10*, 880–889. <https://doi.org/10.1002/adma.200400767>.
35. Nishioka, K.; Hirakawa, K. Fundamental Investigations of Fretting Fatigue: Part 5, The Effect of Relative Slip Amplitude. *Bull. JSME* **1969**, *12*, 692–697.
36. Juuma, T. Torsional Fretting Fatigue Strength of a Shrink-Fitted Shaft. *Wear* **1999**, *231*, 310–318. [https://doi.org/10.1016/S0043-1648\(99\)00249-5](https://doi.org/10.1016/S0043-1648(99)00249-5).
37. Juuma, T. Torsional Fretting Fatigue Strength of a Shrink-Fitted Shaft with a Grooved Hub. *Tribol. Int.* **2000**, *33*, 537–543. [https://doi.org/10.1016/S0301-679X\(00\)00102-X](https://doi.org/10.1016/S0301-679X(00)00102-X).
38. Hirakawa, K.; Toyama, K.; Kubota, M. The Analysis and Prevention of Failure in Railway Axles. *Int. J. Fatigue* **1998**, *20*, 135–144. [https://doi.org/10.1016/S0142-1123\(97\)00096-0](https://doi.org/10.1016/S0142-1123(97)00096-0).
39. Nilsson, F. A Consistent Few Parameter Crack Growth Description Procedure. *Int. J. Fract.* **1992**, *54*, 35–44. <https://doi.org/10.1007/BF00040854>.
40. Riemelmoser, F.O.; Pippin, R. Consideration of the Mechanical Behaviour of Small Fatigue Cracks. *Int. J. Fract.* **2002**, *118*, 251–270. <https://doi.org/10.1023/A:1022928722764>.
41. Cadario, A.; Alfredsson, B. Fatigue Growth of Short Cracks in Ti-17: Experiments and Simulations. *Eng. Fract. Mech.* **2007**, *74*, 2293–2310. <https://doi.org/10.1016/j.engfracmech.2006.11.016>.
42. Lanoue, F.; Vadean, A.; Sanschagrín, B. Finite Element Analysis and Contact Modelling Considerations of Interference Fits for Fretting Fatigue Strength Calculations. *Simul. Model. Pract. Theory* **2009**, *17*, 1587–1602. <https://doi.org/10.1016/j.simpat.2009.06.017>.
43. Lanoue, F.; Vadean, A.; Sanschagrín, B. Fretting Fatigue Strength Reduction Factor for Interference Fits. *Simul. Model. Pract. Theory* **2011**, *19*, 1811–1823. <https://doi.org/10.1016/j.simpat.2011.05.004>.
44. Linhart, V.; Černý, I. An Effect of Strength of Railway Axle Steels on Fatigue Resistance under Press Fit. *Eng. Fract. Mech.* **2011**, *78*, 731–741. <https://doi.org/10.1016/j.engfracmech.2010.11.023>.
45. Song, C.; Shen, M.X.; Lin, X.F.; Liu, D.W.; Zhu, M.H. An Investigation on Rotatory Bending Fretting Fatigue Damage of Railway Axles. *Fatigue Fract. Eng. Mater. Struct.* **2014**, *37*, 72–84. <https://doi.org/10.1111/ffe.12085>.
46. Luke, M.; Burdack, M.; Moroz, S.; Varfolomeev, I. Experimental and Numerical Study on Crack Initiation under Fretting Fatigue Loading. *Int. J. Fatigue* **2016**, *86*, 24–33. <https://doi.org/10.1016/j.ijfatigue.2015.09.022>.
47. Crococolo, D.; De Agostinis, M.; Olmi, G. Fatigue life characterisation of interference fitted joints. In *ASME International Mechanical Engineering Congress and Exposition, Proceedings (IMECE)*; American Society of Mechanical Engineers: New York, NY, USA, 2013; Volume 2B. <https://doi.org/10.1115/IMECE2013-63515>.
48. Crococolo, D.; De Agostinis, M.; Fini, S.; Morri, A.; Olmi, G. Analysis of the Influence of Fretting on the Fatigue Life of Interference Fitted Joints. In *ASME International Mechanical Engineering Congress and Exposition, Proceedings (IMECE)*; American Society of Mechanical Engineers: New York, NY, USA, 2014; Volume 2B. <https://doi.org/10.1115/IMECE2014-38128>.
49. Lykins, C.D.; Mall, S.; Jain, V. Evaluation of Parameters for Predicting Fretting Fatigue Crack Initiation. *Int. J. Fatigue* **2000**, *22*, 703–716. [https://doi.org/10.1016/S0142-1123\(00\)00036-0](https://doi.org/10.1016/S0142-1123(00)00036-0).
50. Smith, K.N.; Topper, T.H.; Watson, P. A Stress–Strain Function for the Fatigue of Metals (Stress–Strain Function for Metal Fatigue Including Mean Stress Effect). *J. Mater.* **1970**, *5*, 767–778.
51. Fatemi, A.; Socie, D.F. A Critical Plane Approach To Multiaxial Fatigue Damage Including Out-of-Phase Loading. *Fatigue Fract. Eng. Mater. Struct.* **1988**, *11*, 149–165. <https://doi.org/10.1111/j.1460-2695.1988.tb01169.x>.
52. Nowell, D.; Hills, D.A.; O’Connor, J.J. Analysis of Fretting Fatigue. *I Mech E Conf. Publ.* **1987**, *5*, 965–973.
53. Zhang, Y.; Lu, L.; Gong, Y.; Zhang, J.; Zeng, D. Fretting Wear-Induced Evolution of Surface Damage in Press-Fitted Shaft. *Wear* **2017**, *384–385*, 131–141. <https://doi.org/10.1016/j.wear.2017.05.014>.
54. Zhang, Y.B.; Lu, L.T.; Zou, L.; Zeng, D.F.; Zhang, J.W. Finite Element Simulation of the Influence of Fretting Wear on Fretting Crack Initiation in Press-Fitted Shaft under Rotating Bending. *Wear* **2018**, *400–401*, 177–183. <https://doi.org/10.1016/j.wear.2018.01.008>.

55. Zeng, D.; Zhang, Y.; Lu, L.; Zou, L.; Zhu, S. Fretting Wear and Fatigue in Press-Fitted Railway Axle: A Simulation Study of the Influence of Stress Relief Groove. *Int. J. Fatigue* **2019**, *118*, 225–236. <https://doi.org/10.1016/j.ijfatigue.2018.09.008>.
56. Fouvry, S.; Liskiewicz, T.; Kapsa, P.; Hannel, S.; Sauger, E. An Energy Description of Wear Mechanisms and Its Applications to Oscillating Sliding Contacts. *Wear* **2003**, *255*, 287–298. [https://doi.org/10.1016/S0043-1648\(03\)00117-0](https://doi.org/10.1016/S0043-1648(03)00117-0).
57. Ince, A.; Glinka, G. A Modification of Morrow and Smith-Watson-Topper Mean Stress Correction Models. *Fatigue Fract. Eng. Mater. Struct.* **2011**, *34*, 854–867. <https://doi.org/10.1111/j.1460-2695.2011.01577.x>.
58. Boddington, P.H.B.; Ruiz, C. A Biaxial Fatigue Test for Dovetail Joints. In Proceedings of the ASME International Conference on Advances of Life Prediction Methods, Albany, NY, USA, 18–20 April 1983.
59. Ruiz, C.; Boddington, P.H.B.; Chen, K.C. An Investigation of Fatigue and Fretting in a Dovetail Joint. *Exp. Mech.* **1984**, *24*, 208–217. <https://doi.org/10.1007/BF02323167>.
60. Boddington, P.H.B.; Chen, K.; Ruiz, C. The Numerical Analysis of Dovetail Joints. *Comput. Struct.* **1985**, *20*, 731–735. [https://doi.org/10.1016/0045-7949\(85\)90034-3](https://doi.org/10.1016/0045-7949(85)90034-3).
61. Titanium, I.M.I. 829. *Trade Publication, Imperial Metal Industries*; Springer: Witton, Birmingham, UK, 1980.
62. He, M.J.; Ruiz, C. Fatigue Life of Dovetail Joints: Verification of a Simple Biaxial Model. *Exp. Mech.* **1989**, *29*, 126–131. <https://doi.org/10.1007/BF02321364>.
63. Papanikos, P.; Meguid, S.A. Theoretical and Experimental Studies of Fretting-Initiated Fatigue Failure of Aeroengine Compressor Discs. *Fatigue Fract. Eng. Mater. Struct.* **1994**, *17*, 539–550. <https://doi.org/10.1111/j.1460-2695.1994.tb00253.x>.
64. Erdogan, F.; Sih, G.C. On the Crack Extension in Plates Under Plane Loading and Transverse Shear. *J. Basic Eng.* **1963**, *85*, 519–525. <https://doi.org/10.1115/1.3656897>.
65. Hutson, A.L.; Nicholas, T.; Goodman, R. Fretting Fatigue of Ti–6Al–4V under Flat-on-Flat Contact. *Int. J. Fatigue* **1999**, *21*, 663–669.
66. Ciavarella, M.; Hills, D.A.; Monno, G. The Influence of Rounded Edges on Indentation by a Flat Punch. *Proc. Inst. Mech. Eng. Part C J. Mech. Eng. Sci.* **1998**, *212*, 319–327. <https://doi.org/10.1243/0954406981521259>.
67. Ciavarella, M.; Demelio, G. A Review of Analytical Aspects of Fretting Fatigue, with Extension to Damage Parameters, and Application to Dovetail Joints. *Internat. J. Solids Struct.* **2001**, *38*, 1791–1811.
68. Ciavarella, M.; Macina, G.; Demelio, G.P. On Stress Concentration on Nearly Flat Contacts. *J. Strain Anal. Eng. Des.* **2002**, *37*, 493–501. <https://doi.org/10.1243/030932402320950116>.
69. Fridrici, V.; Fouvry, S.; Kapsa, P.H. Fretting Wear Behavior of a Cu-Ni-In Plasma Coating. *Surf. Coat. Technol.* **2003**, *163–164*, 429–434. [https://doi.org/10.1016/S0257-8972\(02\)00639-4](https://doi.org/10.1016/S0257-8972(02)00639-4).
70. Conner, B.P.; Lindley, T.C.; Nicholas, T.; Suresh, S. Application of a Fracture Mechanics Based Life Prediction Method for Contact Fatigue. *Int. J. Fatigue* **2004**, *26*, 511–520. <https://doi.org/10.1016/j.ijfatigue.2003.09.003>.
71. Giannakopoulos, A.E.; Lindley, T.C.; Suresh, S. Aspects of Equivalence between Contact Mechanics and Fracture Mechanics: Theoretical Connections and a Life-Prediction Methodology for Fretting-Fatigue. *Acta Mater.* **1998**, *46*, 2955–2968. [https://doi.org/10.1016/S1359-6454\(98\)00011-1](https://doi.org/10.1016/S1359-6454(98)00011-1).
72. Conner, B.P.; Nicholas, T. Using a Dovetail Fixture to Study Fretting Fatigue and Fretting Palliatives. *J. Eng. Mater. Technol. Trans. ASME* **2006**, *128*, 133–141. <https://doi.org/10.1115/1.2172272>.
73. Murthy, H.; Harish, G.; Farris, T.N. Efficient Modeling of Fretting of Blade/Disk Contacts Including Load History Effects. *J. Tribol.* **2004**, *126*, 56–64. <https://doi.org/10.1115/1.1540125>.
74. Golden, P.J.; Nicholas, T. The Effect of Angle on Dovetail Fretting Experiments in Ti-6Al-4V. *Fatigue Fract. Eng. Mater. Struct.* **2005**, *28*, 1169–1175. <https://doi.org/10.1111/j.1460-2695.2005.00956.x>.
75. Calcaterra, J.; Naboulsi, S. Design Methodology to Investigate Contact Fatigue Damage in Turbine Engine Hardware. *Int. J. Fatigue* **2005**, *27*, 1133–1141. <https://doi.org/10.1016/j.ijfatigue.2005.01.012>.
76. Golden, P.J.; Calcaterra, J.R. A Fracture Mechanics Life Prediction Methodology Applied to Dovetail Fretting. *Tribol. Int.* **2006**, *39*, 1172–1180. <https://doi.org/10.1016/j.triboint.2006.02.006>.
77. Golden, P.J.; Shepard, M.J. Life Prediction of Fretting Fatigue with Advanced Surface Treatments. *Mater. Sci. Eng. A* **2007**, *468–470*, 15–22. <https://doi.org/10.1016/j.msea.2006.10.168>.
78. Bartha, B.B.; Nicholas, T.; Farris, T.N. Modeling of Geometry Effects in Fretting Fatigue. *Tribol. Int.* **2006**, *39*, 1131–1141. <https://doi.org/10.1016/j.triboint.2006.02.003>.
79. Golden, P.J.; Hutson, A.L.; Bartha, B.B.; Nicholas, T. Fatigue Loading and Life Prediction in Three Fretting Fatigue Fixtures. *Exp. Mech.* **2008**, *48*, 253–263. <https://doi.org/10.1007/s11340-008-9130-8>.
80. Golden, P.J. Development of a Dovetail Fretting Fatigue Fixture for Turbine Engine Materials. *Int. J. Fatigue* **2009**, *31*, 620–628. <https://doi.org/10.1016/j.ijfatigue.2008.03.017>.
81. Anandavel, K.; Prakash, R.V. Effect of Three-Dimensional Loading on Macroscopic Fretting Aspects of an Aero-Engine Bladedisc Dovetail Interface. *Tribol. Int.* **2011**, *44*, 1544–1555. <https://doi.org/10.1016/j.triboint.2010.10.014>.
82. Anandavel, K.; Prakash, R.V. Extension of Ruiz Criterion for Evaluation of 3-D Fretting Fatigue Damage Parameter. *Procedia Eng.* **2013**, *55*, 655–660. <https://doi.org/10.1016/j.proeng.2013.03.310>.
83. Murugesan, J.; Mutoh, Y. Fretting Fatigue Strength Prediction of Dovetail Joint and Bolted Joint by Using the Generalized Tangential Stress Range-Compressive Stress Range Diagram. *Tribol. Int.* **2014**, *76*, 116–121. <https://doi.org/10.1016/j.triboint.2013.11.006>.

84. Mutoh, Y.; Jayaprakash, M. Tangential Stress Ranges/Compressive Stress Range Diagram for Fretting Fatigue Design Curve. *Tribol. Int.* **2011**, *44*, 1394–1399. <https://doi.org/10.1016/j.triboint.2010.10.013>.
85. Chaboche, J.L. Constitutive Equations for Cyclic Plasticity and Cyclic Viscoplasticity. *Int. J. Plast.* **1989**, *5*, 247–302. [https://doi.org/10.1016/0749-6419\(89\)90015-6](https://doi.org/10.1016/0749-6419(89)90015-6).
86. Shi, L.; Wei, D.S.; Wang, Y.R.; Tian, A.M.; Li, D. An Investigation of Fretting Fatigue in a Circular Arc Dovetail Assembly. *Int. J. Fatigue* **2016**, *82*, 226–237. <https://doi.org/10.1016/j.ijfatigue.2015.07.025>.
87. Araújo, J.A.; Nowell, D. The Effect of Rapidly Varying Contact Stress Fields on Fretting Fatigue. *Int. J. Fatigue* **2002**, *24*, 763–775. [https://doi.org/10.1016/S0142-1123\(01\)00191-8](https://doi.org/10.1016/S0142-1123(01)00191-8).
88. Naboulsi, S.; Mall, S. Fretting Fatigue Crack Initiation Behavior Using Process Volume Approach and Finite Element Analysis. *Tribol. Int.* **2003**, *36*, 121–131. [https://doi.org/10.1016/S0301-679X\(02\)00139-1](https://doi.org/10.1016/S0301-679X(02)00139-1).
89. Yang, Q.; Zhou, W.; Gai, P.; Zhang, X.; Fu, X.; Chen, G.; Li, Z. Investigation on the Fretting Fatigue Behaviors of Ti-6Al-4V Dovetail Joint Specimens Treated with Shot-Peening. *Wear* **2017**, *372–373*, 81–90. <https://doi.org/10.1016/j.wear.2016.12.004>.
90. Mangardich, D.; Abrari, F.; Fawaz, Z. A Fracture Mechanics Based Approach for the Fretting Fatigue of Aircraft Engine Fan Dovetail Attachments. *Int. J. Fatigue* **2019**, *129*, 105213. <https://doi.org/10.1016/j.ijfatigue.2019.105213>.
91. Ding, J.; Sum, W.S.; Sabesan, R.; Leen, S.B.; McColl, I.R.; Williams, E.J. Fretting Fatigue Predictions in a Complex Coupling. *Int. J. Fatigue* **2007**, *29*, 1229–1244. <https://doi.org/10.1016/j.ijfatigue.2006.10.017>.
92. Sandifer, J.P. Evaluation of Methods for Reducing Fretting Fatigue Damage in 2024-T3 Aluminium Lap Joints. *Wear* **1973**, *26*, 405–412.
93. Wagle, S.; Kato, H. Ultrasonic Detection of Fretting Fatigue Damage at Bolt Joints of Aluminum Alloy Plates. *Int. J. Fatigue* **2009**, *31*, 1378–1385. <https://doi.org/10.1016/j.ijfatigue.2009.03.017>.
94. Zografos, A.; Dini, D.; Olver, A.V. Fretting Fatigue and Wear in Bolted Connections: A Multi-Level Formulation for the Computation of Local Contact Stresses. *Tribol. Int.* **2009**, *42*, 1663–1675. <https://doi.org/10.1016/j.triboint.2009.03.007>.
95. Jayaprakash, M.; Mutoh, Y.; Yoshii, K. Fretting Fatigue Behavior and Life Prediction of Automotive Steel Bolted Joint. *Mater. Des.* **2011**, *32*, 3911–3919. <https://doi.org/10.1016/j.matdes.2011.02.061>.
96. Mutoh, Y.; Jayaprakash, M.; Asai, K.; Ichikawa, K. Effect of Contact Pad Rigidity and Fretting Fatigue Design Curve. *Trans. Indian Inst. Met.* **2010**, *63*, 181–186. <https://doi.org/10.1007/s12666-010-0025-x>.
97. Chakherlou, T.N.; Razavi, M.J.; Aghdam, A.B.; Abazadeh, B. An Experimental Investigation of the Bolt Clamping Force and Friction Effect on the Fatigue Behavior of Aluminum Alloy 2024-T3 Double Shear Lap Joint. *Mater. Des.* **2011**, *32*, 4641–4649. <https://doi.org/10.1016/j.matdes.2011.04.022>.
98. Eriten, M.; Polycarpou, A.A.; Bergman, L.A. Physics-Based Modeling for Fretting Behavior of Nominally Flat Rough Surfaces. *Int. J. Solids Struct.* **2011**, *48*, 1436–1450. <https://doi.org/10.1016/j.ijsolstr.2011.01.028>.
99. Eriten, M.; Polycarpou, A.A.; Bergman, L.A. Development of a Lap Joint Fretting Apparatus. *Exp. Mech.* **2011**, *51*, 1405–1419. <https://doi.org/10.1007/s11340-010-9458-8>.
100. Benhamena, A.; Amrouche, A.; Talha, A.; Benseddiq, N. Effect of Contact Forces on Fretting Fatigue Behavior of Bolted Plates: Numerical and Experimental Analysis. *Tribol. Int.* **2012**, *48*, 237–245. <https://doi.org/10.1016/j.triboint.2011.12.008>.
101. Oskouei, R.H.; Ibrahim, R.N. Improving Fretting Fatigue Behaviour of Al 7075-T6 Bolted Plates Using Electroless Ni-P Coatings. *Int. J. Fatigue* **2012**, *44*, 157–167. <https://doi.org/10.1016/j.ijfatigue.2012.05.003>.
102. Ferjaoui, A.; Yue, T.; Abdel Wahab, M.; Hojjati-Talemi, R. Prediction of Fretting Fatigue Crack Initiation in Double Lap Bolted Joint Using Continuum Damage Mechanics. *Int. J. Fatigue* **2015**, *73*, 66–76. <https://doi.org/10.1016/j.ijfatigue.2014.11.012>.
103. *ASTM E2789-10*; Standard Guide for Fretting Fatigue Testing. ASTM International: West Conshohocken, PA, USA, 2015; Volume 10, pp. 1–10. <https://doi.org/10.1520/E2789>.
104. Jiménez-Peña, C.; Talemi, R.H.; Rossi, B.; Debruyne, D. Investigations on the Fretting Fatigue Failure Mechanism of Bolted Joints in High Strength Steel Subjected to Different Levels of Pre-Tension. *Tribol. Int.* **2017**, *108*, 128–140. <https://doi.org/10.1016/j.triboint.2016.11.014>.
105. Crossland, B. Effect of Large Hydrostatic Pressures on the Torsional Fatigue Strength of an Alloy Steel. In Proceedings of the International Conference on Fatigue of Metals, London, UK, 10–14 September 1956, New York, NY, USA, 28–30 November 1956; pp. 138–149.
106. Vingsbo, O.; Söderberg, S. On Fretting Maps. *Wear* **1988**, *126*, 131–147.
107. Venugopal Poovakaud, V.; Jiménez-Peña, C.; Talemi, R.; Coppieters, S.; Debruyne, D. Assessment of Fretting Fatigue in High Strength Steel Bolted Connections with Simplified Fe Modelling Techniques. *Tribol. Int.* **2020**, *143*, 106083. <https://doi.org/10.1016/j.triboint.2019.106083>.
108. Mäntylä, A.; Hintikka, J.; Frondelius, T.; Vaara, J.; Lehtovaara, A.; Juoksukangas, J. Prediction of Contact Condition and Surface Damage by Simulating Variable Friction Coefficient and Wear. *Tribol. Int.* **2020**, *143*, 106054. <https://doi.org/10.1016/j.triboint.2019.106054>.
109. Juoksukangas, J.; Nurmi, V.; Hintikka, J.; Vippola, M.; Lehtovaara, A.; Mäntylä, A.; Vaara, J.; Frondelius, T. Characterization of Cracks Formed in Large Flat-on-Flat Fretting Contact. *Int. J. Fatigue* **2019**, *124*, 361–370. <https://doi.org/10.1016/j.ijfatigue.2019.03.004>.
110. Mäntylä, A.; Juoksukangas, J.; Hintikka, J.; Frondelius, T.; Lehtovaara, A. FEM-Based Wear Simulation for Fretting Contacts. *Raken. Mek.* **2020**, *53*, 20–27. <https://doi.org/10.23998/rm.76261>.

111. Juoksukangas, J.; Lehtovaara, A.; Mäntylä, A. Experimental and Numerical Investigation of Fretting Fatigue Behavior in Bolted Joints. *Tribol. Int.* **2016**, *103*, 440–448. <https://doi.org/10.1016/j.triboint.2016.07.021>.
112. Hintikka, J.; Mäntylä, A.; Vaara, J.; Frondelius, T.; Juoksukangas, J.; Lehtovaara, A. Running-in in Fretting, Transition from near-Stable Friction Regime to Gross Sliding. *Tribol. Int.* **2020**, *143*, 106073. <https://doi.org/10.1016/j.triboint.2019.106073>.
113. Juoksukangas, J.; Nurmi, V.; Hintikka, J.; Honkanen, M.; Vippola, M.; Lehtovaara, A.; Mäntylä, A.; Vaara, J.; Frondelius, T. Cracks and Degradation Layers in Large Flat-on-Flat Fretting Contact with Steels and Cast Iron. *Tribol. Int.* **2020**, *145*, 106102. <https://doi.org/10.1016/j.triboint.2019.106102>.
114. Zhou, Z.R.; Fayeulle, S.; Vincent, L. Cracking Behaviour of Various Aluminium Alloys during Fretting Wear. *Wear* **1992**, *155*, 317–330. [https://doi.org/10.1016/0043-1648\(92\)90091-L](https://doi.org/10.1016/0043-1648(92)90091-L).
115. Zhou, Z.; Vincent, L. Mixed Fretting Regime. *Wear* **1995**, *181*, 531–536.
116. Zhou, Z.R.; Nakazawa, K.; Zhu, M.H.; Maruyama, N.; Kapsa, P.; Vincent, L. Progress in Fretting Maps. *Tribol. Int.* **2006**, *39*, 1068–1073. <https://doi.org/10.1016/j.triboint.2006.02.001>.